

## New methodology for deriving total ozone and other atmospheric variables from Brewer spectrophotometer direct sun spectra

J. B. Kerr

Meteorological Service of Canada, Environment Canada, Downsview, Ontario, Canada

Received 17 August 2001; revised 28 December 2001; accepted 8 January 2002; published 14 December 2002.

[1] A new method has been developed for taking high-quality spectral measurements of ultraviolet radiation with the Brewer spectrophotometer. Spectral measurements of direct solar radiation made routinely with the new method at Toronto between 1996 and 2001 were used to determine total ozone, aerosol optical depth, sulfur dioxide and ozone temperature. Corrections to laboratory-based ozone absorption coefficients have been derived from the data set of these new measurements as have the temperature dependencies of standard Brewer and Dobson total ozone measurements. It was found that the temperature of atmospheric ozone has little effect on the total ozone derived from the standard algorithm used for the Brewer instrument. The new measurement method and the calibration information required to derive the atmospheric variables from the spectra are described. Results of calibrations carried out at Mauna Loa Observatory in 1997 and 2000 are presented. The records of atmospheric variables measured at Toronto between 1996 and 2001 are given. *INDEX TERMS*: 0305 Atmospheric Composition and Structure: Aerosols and particles (0345, 4801); 0360 Atmospheric Composition and Structure: Transmission and scattering of radiation; 0394 Atmospheric Composition and Structure: Instruments and techniques; 3360 Meteorology and Atmospheric Dynamics: Remote sensing; *KEYWORDS*: total ozone, ozone temperature, aerosol optical depth, spectral measurements, solar radiation

**Citation:** Kerr, J. B., New methodology for deriving total ozone and other atmospheric variables from Brewer spectrophotometer direct sun spectra, *J. Geophys. Res.*, 107(D23), 4731, doi:10.1029/2001JD001227, 2002.

### 1. Introduction

[2] Ozone absorbs radiation strongly in the ultraviolet (UV) and for wavelengths less than 315 nm the absorption increases rapidly with decreasing wavelength. The total column amount of atmospheric ozone has been routinely measured from the ground for a few decades at many sites with Dobson and Brewer spectrophotometers and ozonometer filter instruments using the sharp gradient of ozone absorption in this wavelength region of the solar spectrum. All of these instruments use differential absorption techniques where, in principle, the measured intensity of radiation at a wavelength with strong ozone absorption (shorter wavelength) is compared with that at a wavelength with significantly less ozone absorption (longer wavelength). In addition, satellite instruments such as the total ozone mapping spectrometer (TOMS) measure ozone from space using similar differential absorption techniques in the UV. These instruments have single detectors and the radiation at the different wavelengths is optically selected. The filter instruments, which are extensively used in countries of the former USSR, use a pair of wavelengths [Gustin *et al.*, 1985], Dobson instruments use double pairs of wavelengths to

reduce effects of atmospheric aerosols [Dobson, 1957] and Brewer instruments use a set of 5 operational wavelengths to reduce the effects of aerosols and to measure sulphur dioxide [Kerr *et al.*, 1981].

[3] The wavelength dependence of radiation scattered by atmospheric aerosols or thin clouds is relatively small over the UV-B wavelength region (280 nm to 315 nm) of the solar spectrum. Measurement of the aerosol optical depth (AOD) is therefore considerably more difficult than that of ozone since differential techniques should not be applied because results are very uncertain and measurements on an absolute scale must be used. Also the fact that ozone absorbs strongly in this spectral region must be considered in the retrieval of AOD values. Optical depth values are determined from measurements of the direct solar radiation, where the term direct solar refers to radiation arriving at an instrument only from the direction of the Sun. It has been demonstrated that operational direct sun observations made at the 5 standard wavelengths of the Brewer instrument can be used to determine AOD over long periods of time [Kerr, 1997; Carvalho and Henriques, 2000; Jaroslowski and Krzyscin, 2000; Kirchhoff *et al.*, 2001; Gröbner *et al.*, 2001].

[4] The availability of array detectors has led to the development of multidetector spectral instruments that are used in the UV and visible regions of the solar spectrum to detect atmospheric constituents [e.g., Hofmann *et al.*, 1995].

**Table 1.** Wavelengths and FWHI Resolutions of the Group Scan for Brewer Instrument 14

Group	Micrometer Setting	Slit 1 Wavelength (Resolution)	Slit 2 Wavelength (Resolution)	Slit 3 Wavelength (Resolution)	Slit 4 Wavelength (Resolution)	Slit 5 Wavelength (Resolution)
1	3667	306.3603 (0.5937)	310.0959 (0.5848)	313.5410 (0.6139)	316.8332 (0.5951)	320.0397 (0.5778)
2	3736	306.8327 (0.5937)	310.5624 (0.5847)	314.0020 (0.6136)	317.2886 (0.5947)	320.4896 (0.5773)
3	3813	307.3595 (0.5938)	311.0826 (0.5845)	314.5158 (0.6133)	317.7963 (0.5942)	320.9911 (0.5767)
4	3890	307.8856 (0.5938)	311.6021 (0.5843)	315.0291 (0.6129)	318.3034 (0.5937)	321.4920 (0.5760)
5	3967	308.4112 (0.5938)	312.1211 (0.5841)	315.5418 (0.6126)	318.8099 (0.5931)	321.9924 (0.5753)
6	4044	308.9362 (0.5937)	312.6395 (0.5839)	316.0539 (0.6121)	319.3159 (0.5926)	322.4922 (0.5745)
7	4122	309.4674 (0.5936)	313.1640 (0.5835)	316.5721 (0.6117)	319.8279 (0.5919)	322.9979 (0.5737)
8	4199	309.9912 (0.5934)	313.6813 (0.5832)	317.0831 (0.6111)	320.3326 (0.5912)	323.4965 (0.5729)
9	4277	310.5213 (0.5932)	314.2047 (0.5828)	317.6001 (0.6106)	320.8434 (0.5905)	324.0010 (0.5720)

These instruments sample radiation at many wavelengths simultaneously. This is advantageous since complete spectra over a targeted wavelength range are measured in a relatively short time and variability in observing conditions (caused by fluctuations in thin clouds or aerosols) has minimal impact on the shape of the spectra. Consequently, small variations in spectral features ( $\sim 0.1\%$ ) can be detected, allowing the identification and quantification of small concentrations of trace species.

[5] In general, a spectrum of sunlight measured below or within the atmosphere may be used to determine atmospheric constituents by the differential optical absorption spectroscopy (DOAS) analysis technique [Solomon *et al.*, 1987]. The DOAS technique requires knowledge of a reference spectrum and the spectra of absorption cross sections of atmospheric species. For the case of direct solar spectral measurements the reference spectrum is usually the extraterrestrial (ET) spectrum (log of direct sun readings that the instrument would measure outside the atmosphere). Atmospheric constituents are determined by least square fitting an observed absorption spectrum (ET spectrum minus the log of the readings on the direct sun corrected for the known attenuation due to Rayleigh scattering) to a number of vectors which include the absorption spectra of atmospheric species, a constant offset and a linear slope with wavelength. Column values of absorbing gases in the atmosphere are determined from the coefficients of the fit to the appropriate absorption spectrum. Aerosol optical depth is derived from the constant offset and linear dependence coefficients of the fit. Residuals remaining from the fit give an indication of the quality of measurement and provide an uncertainty estimate for each atmospheric constituent.

[6] This paper presents a new method of measurement that allows the Brewer instrument to take good quality full spectra over a targeted spectral range. The spectra are analyzed with a modified DOAS technique that quantifies and corrects for variability that occurs during the course of scans. The new (group-scan) method is described, requirements for calibration are discussed and a 4-year record of measurements is given.

## 2. Group-Scan Method

[7] Operational direct sun measurements made by the Brewer spectrophotometer use direct solar radiation at five fixed wavelengths in the UV, nominally 306.3 nm, 310.0 nm, 313.5 nm, 316.8 nm and 320.0 nm, with a full-width-half-intensity (FWHI) resolution of about 0.6nm. The five wavelengths are defined by five exit slits at approximate

uniform spacing ( $3.5 \pm 0.3$  nm) along the focal plane of the spectrometer. Radiation from the five wavelengths is sequentially and repeatedly sampled quite rapidly (40 times each in 35 seconds) by a blocking mask that is positioned by a stepper motor. This rapid sampling repeated many times in one observation results in essentially simultaneous measurements being made at the five wavelengths, so changing conditions that affect all wavelengths equally during the sampling period generally have little impact on total ozone values derived from the differential absorption technique.

[8] Operational UV-B spectral measurements are made with the Brewer instrument in the traditional wavelength scanning mode that rotates the grating [Kerr and McElroy, 1993]. Radiation passing through one open slit is sampled at discrete grating settings over the appropriate wavelength range. The spectral elements are sampled at different times and significant noise can be generated if this fact is disregarded in analysis, as it often is.

[9] The new group-scan method developed for the Brewer instrument combines the rapid sampling of the five wavelengths with the slower spectral scanning that is traditionally carried out by rotating the grating. All five slits are sampled at nine grating settings, starting with the normal position and stepping by approximately 0.5 nm, so that the spaces between the five operational wavelengths are filled. Values of the 45 wavelengths (five slits times nine grating positions) and their FWHI resolutions are given in Table 1. Scans are done in the forward direction followed by the backward direction so that all 45 scan elements can be interpolated to a common airmass value. The total scan takes about 2.5 minutes. This sampling technique has the advantage that the complete spectral range (306.3 nm to 324.0 nm) is sampled at 45 wavelengths offering the opportunity to identify and quantify spectral features attributable to absorbing atmospheric gases.

[10] Spectra observed with the group-scan method are analyzed by a modified version of the DOAS analysis technique. The main difference between the normal DOAS technique and the new technique is the treatment of variability in observing conditions from one of the nine groups of five wavelengths to another. This is done by assuming that the main source of variability is due to changes in the optical depth of aerosols or thin clouds and that the variability affects all five wavelengths in a particular group equally. For a scan consisting of all 45 wavelengths, there are assumed to be nine values (one for each group) of aerosol optical depth. Thus changes in observing conditions during the course of the measurements can be quantified

from the variability of the nine aerosol optical depth values and resulting uncertainties for determining atmospheric absorbers are significantly reduced.

[11] The group-scan sampling method has been used to take spectral observations of direct sun, global and zenith sky irradiance at Toronto since November 1996 with Brewer instrument 14, one of the Brewer reference triad [Kerr *et al.*, 1985, 1998]. These observations have been made throughout the day from sunrise to sunset under conditions with a wide range of variables such as total ozone, cloud cover, haze and albedo. The measurements have been included as part of a typical operating schedule that normally takes direct sun, UV-B scan, zenith sky and calibration lamp readings. This study presents results of only the direct sun data set to demonstrate the effectiveness of the technique and show some example results. Analysis of the global and zenith data sets and comparison of the group-scan results with the standard measurements will be the subjects of future studies.

### 3. Instrumental Corrections

[12] There are a number of corrections that must be applied to the group-scan spectra measured by the Brewer instrument. These include correction of the photon counting signals for dead time and dark count in a similar fashion as the correction is applied to operational measurements. Measurements are made over a range of instrument temperatures with different 'near-neutral density' filters that are used to reduce light intensities to manageable levels. Comparison of spectra taken with different filters and/or temperatures requires corrections to account for the different situations. Both of these corrections are wavelength dependent. Figure 1 shows the filter attenuation values as a function of wavelength for the four filters in Brewer instrument 14. These measurements were made on November 13, 1996 using the internal standard lamp as a light source to determine the attenuation of the four filters. Similar measurements made on March 1, 1999 indicated that the attenuation values and wavelength dependence have been very stable (to within  $\pm 1\%$ ) with time. Figure 2 shows the temperature dependence of the responsivity of the instrument as a function of wavelength. These values are determined from 1882 spectral measurements of the internal standard lamp during 1999 over a temperature range from  $+1^\circ\text{C}$  to  $+39^\circ\text{C}$ . The wavelength dependence of the temperature dependence over this wavelength range has a similar behavior as that measured with Brewer instrument 14 at other times and is similar in shape and within the range of those reported for several other Brewer instruments [Weatherhead *et al.*, 2001]. All measurements reported here have been corrected using the dependence values shown in Figures 1 and 2.

[13] Spectra measured by the single Brewer instrument used in this work include a stray light component that originates from radiation at nearby wavelengths (mostly within  $\pm 40$  nm). Stray light is an important contribution when the radiation at one wavelength is significantly less ( $\sim 1\%$ ) than that at a wavelength which is close enough to produce stray light and far enough away to have different absorption characteristics ( $\sim 10$  nm away). This situation occurs in the 305 nm to 325 nm spectral region since the

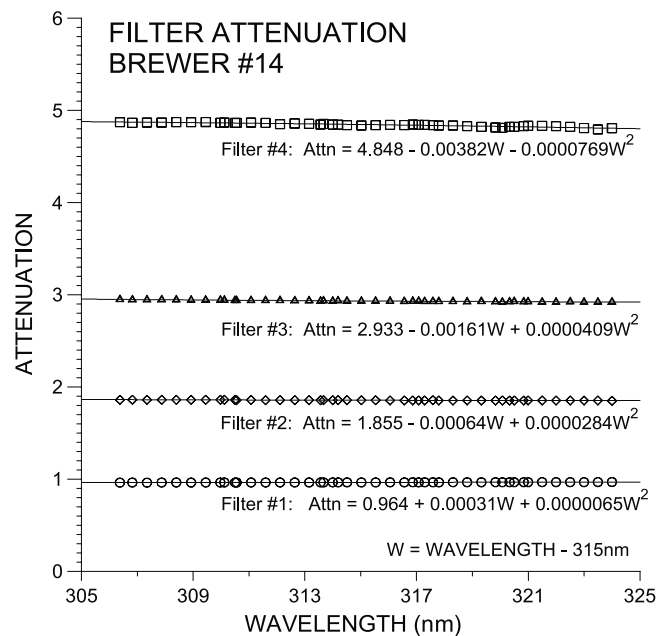


**Figure 1.** Filter attenuation values as functions of wavelength for the four filters of Brewer instrument 14. The plotted data points are measured optical depth values and the lines are quadratic fits to the data points with the fit coefficients indicated for each filter. The first coefficients gives the filter attenuations at 315 nm and the second and third coefficients indicate their wavelength dependence. Measurements were made on November 13, 1996 using the internal standard lamp as a light source.

gradient of ozone absorption is large over this wavelength range. The contribution of stray light becomes more and more significant for shorter wavelengths as the gradient of radiation increases with increasing slant path through atmospheric ozone.

[14] Stray light is corrected using a technique similar to that described by Fioletov *et al.* [2000]. Radiation from the 325 nm line of a helium cadmium laser is scanned with the Brewer instrument to yield a spectrum,  $L(\lambda)$ . Any signal measured by the Brewer instrument at wavelengths more than the FWHI resolution ( $\sim 0.6$  nm) away from the 325 nm laser line is attributable to stray light since the similar out-of-band signal recorded by double spectrometers on these lasers is at least 1000 times smaller [e.g., Wardle *et al.*, 1998]. The function  $\delta(\lambda - 325 \text{ nm}) (= L(\lambda - 325 \text{ nm})/L(325 \text{ nm}))$  is derived for  $|\lambda - 325 \text{ nm}| > 0.6 \text{ nm}$  to quantify the stray light contribution as a function of wavelength away from the source. The stray light spectrum,  $S(\lambda_i)$ , for a measured solar spectrum is then calculated using

$$S(\lambda_i) = \sum_{j=1}^{45} I(\lambda_j) \delta(\lambda_j - \lambda_i) (\lambda_{j+1} - \lambda_{j-1}) / R(\lambda_j) \quad (1)$$

where  $I(\lambda_i)$  is the measured intensity at wavelength  $i$  ( $i = 1$  to 45) and  $R(\lambda_j)$  is the FWHI resolution at  $\lambda_j$ . It should be noted that there is also stray light originating from wavelengths shorter than the first and longer than the last spectral elements. This is accounted for by increasing the weighting

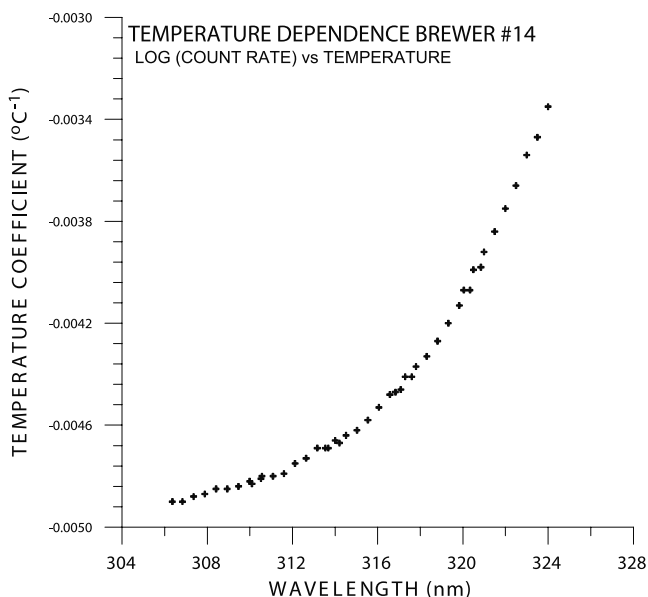


**Figure 2.** Temperature dependence of Brewer instrument 14. Measurements are determined from spectral measurements of the internal lamp made during 1999 over a temperature range between +1 and +39°C.

of the shortest (longest) of the 45 wavelengths to represent stray light from wavelengths shorter (longer) than 306.3 nm (324 nm). The appropriate weighting for contributions from the first and last wavelengths were derived empirically and the first and last wavelengths are not used for the group-scan DOAS least squares fitting analysis. The stray light spectrum,  $S(\lambda_i)$ , is then subtracted from the measured spectrum,  $I(\lambda_i)$  to yield a spectrum corrected for stray light. In practice the procedure is iterated a second time. An example of a measured spectrum, the stray light spectrum, the corrected spectrum and the relative contribution of stray light is shown in Figure 3.

[15] Figure 3 shows that the ratio of the contribution of stray light to the corrected count rate is between 2% and 3% for the wavelengths normally used to calculate total ozone (310 to 320 nm) and increases with increasing ozone absorption (shorter wavelengths). This relative increase of stray light with increasing ozone absorption is the main cause for reduced accuracy of routine direct sun total ozone measurements made with Dobson and single Brewer instruments when the airmass value is larger than 3 to 3.5.

#### 4. Calibrations

[16] Extraterrestrial calibrations of Brewer instruments are carried out regularly at Mauna Loa Observatory (MLO), Hawaii (19.539°N, 155.578°W, 3397 m.a.s.l. altitude) using the Langley plot method. This site offers the stable observing conditions required for the calibrations. The high altitude of MLO is above most tropospheric contamination and the tropical location ensures minimal day-to-day variability of total ozone. The calibrations are done in 2 parts, each lasting about 10 days. Results of the first part are applied to past data and those of the second part are used for future data. Any changes to the instrument (e.g.,

realignment, replacing or cleaning optical components, etc.) are done between the first and second period.

[17] The intensity of direct solar UV radiation at wavelength  $\lambda$  measured at the ground after passing through a cloudless atmosphere is given by

$$I(\lambda) = I_0(\lambda) \exp(-\alpha(\lambda)X\mu - \beta(\lambda)m - \tau_a(\lambda)s) \quad (2)$$

where  $I(\lambda)$  is the measured intensity at wavelength  $\lambda$ ,  $I_0(\lambda)$  is the intensity that would be measured outside the Earth's atmosphere (ET intensity) at  $\lambda$ ,  $\alpha(\lambda)$  is the ozone absorption coefficient at  $\lambda$ ,  $X$  is the total column amount of ozone in the atmosphere,  $\mu$  is the relative slant path through ozone (airmass value),  $\beta(\lambda)$  is the Rayleigh scattering coefficient (those of *Bates* [1984] are used in this work),  $m$  is the number of atmospheres along the slant path,  $\tau_a(\lambda)$  is the aerosol optical depth and  $s$  is the slant path through atmospheric aerosols. It should be noted that  $\mu$  and  $s$  are nearly equal if the height of the aerosols is about the same as that of the ozone layer (i.e., stratospheric aerosols), as is the case with the clean tropospheric conditions normally present at MLO. The wavelength dependence of aerosol optical depth is smooth and essentially linear with wavelength over the relatively small wavelength range used here (363.2 nm to 324.0 nm).

[18] The DOAS analysis requires a reference spectrum to which all measured spectra are compared. In the case of direct solar spectra, the most appropriate reference is the ET solar spectrum which is determined by the zero airmass extrapolation or Langley method [e.g., *Bais*, 1997; *Gröbner and Kerr*, 2001]. Group-scan extrapolation measurements were made with Brewer instrument 14 at MLO in March-April, 1997 and 2000. Spectra are measured over a range of SZAs throughout the day and the log of the measured signal (photon count rate in counts per second corrected for dark count, dead time, neutral density filters, temperature dependence and stray light) plus the known attenuation caused by

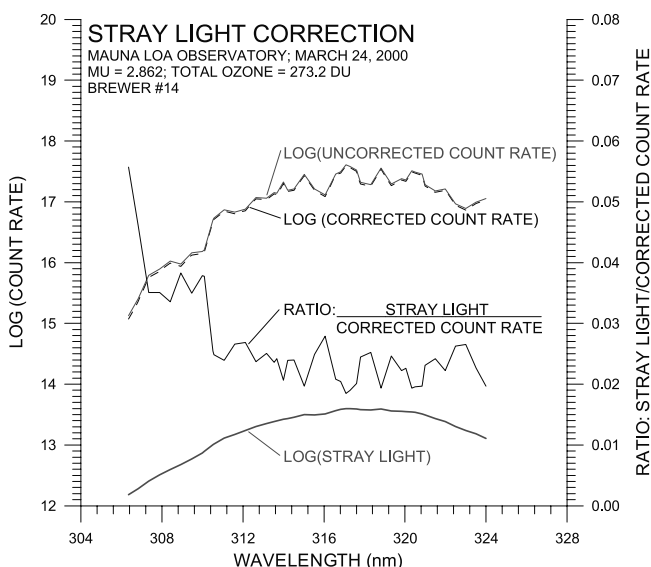


**Figure 3.** Example of stray light correction for a spectrum measured by Brewer instrument 14. The relative contribution of stray light as a function of wavelength is also shown.

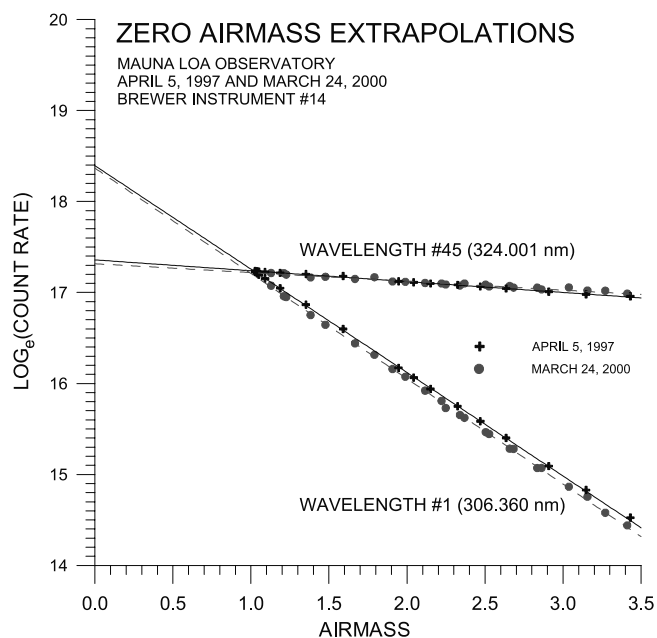


**Figure 4.** Example of Langley extrapolation measurements for the longest and shortest wavelengths of the group scan made at MLO on April 5, 1997 and March 24, 2000.

Rayleigh scattering is plotted against the airmass value,  $\mu$ . With the assumption that  $\mu \approx s$ , it is apparent from (2) that the ET value,  $\log(I_o(\lambda))$ , is the extrapolation of this plot to zero airmass and the attenuation from ozone absorption and aerosol optical depth ( $\alpha(\lambda)X + \tau_a(\lambda)$ ) is the slope. Figure 4 shows examples of airmass extrapolations measured at two wavelengths (306.3 and 324.0 nm) on April 5, 1997 and on March 24, 2000. The average ET values for the 1997 and 2000 calibration periods for all 45 wavelengths are shown in Figure 5. The fact that these two spectra are in good general agreement (mostly within  $\pm 1$  or 2%) indicates that the instrument likely remained quite stable in sensitivity over the three year period. The absolute irradiance of the solar spectra was determined by the same calibration method described by Gröbner and Kerr [2001]. There is good absolute agreement (to within  $\pm 1-2\%$ ) between the results measured here and those of Gröbner and Kerr, who used a double Brewer monochromator. Good agreement was also observed with the spaced-based measurements made with the Solar Ultraviolet Spectral Irradiance Monitor (SUSIM) on the third Atmospheric Laboratory for Applications and Science (ATLAS-3) Space Shuttle mission [VanHoosier, 1996] and smoothed to the resolution of the Brewer instrument. It should be noted that all direct irradiance data reported here have been adjusted to account for variations in the Sun-Earth distance.

[19] In operation, analysis of solar spectra using the DOAS technique is complicated by the fact that instruments do not necessarily remain stable from one scan to another, particularly over an extended period of time (several months) or over a range of operating temperatures. Small relative movements ( $< \sim .001$  mm) of optical components can change the alignment and focus of a spectrometer causing detectable variations of wavelength setting, dispersion and spectral resolution. It is important to keep these

optical properties as stable as possible since the solar spectrum is highly structured and any optical change can lead to a significant change in measured radiation at a particular wavelength setting. For example, with the resolution of the Brewer instrument, an error of about  $\pm 1\%$  would be generated by a wavelength change of  $\pm 0.02$  nm at most wavelength settings. The wavelength-to-wavelength differences between the 1997 and 2000 ET spectra shown in Figure 5 are likely due to minute changes in the instrument's slit functions or relative wavelength settings.

[20] Knowledge of the local shape (slope and curvature) of the solar spectrum near the 45 wavelength settings allows the measurement of and correction for differences (or shifts) in wavelength that may occur between a spectrum measured in Toronto and the reference spectrum measured at a different time at MLO. In order to determine the local shape of the solar spectrum, over-sampled scans were made under clear conditions near local noon at MLO during the calibration periods. The scans comprised 11 measurements at increments of 0.0014 nm (2 micrometer steps [ms]) between  $-0.007$  and  $+0.007$  nm ( $-10$  and  $+10$  ms) about each of the 45 wavelength settings. After appropriate adjustment for Rayleigh scattering and ozone absorption, the 45 sets of 11 data points ( $\log(I_o(\lambda_i, ms))$ ;  $i = 1$  to 45;  $ms = (-5$  to  $+5) * 2$ ) were used to determine the local shapes about the 45 ET values shown in Figure 5. Second order polynomials ( $\log(I_o(\lambda_i, ms)) = a_i + b_i * ms + c_i * ms^2$ ) were fit to the data to determine the local slopes ( $b_i$ 's; shown in Figure 6) and curvatures ( $c_i$ 's; shown in Figure 7) for both calibration periods. The 45 slope values ( $b_i = \Delta \log(I_o(\lambda_i)) / \Delta ms$ ) are used as a vector in the DAOS fitting technique to determine the wavelength shift ( $\delta ms$ ) between a measured spectrum and the reference spectrum. The reference spectrum is then adjusted by adding ( $b_i * \delta ms + c_i * (\delta ms)^2$ ).

[21] The DOAS technique also requires accurate knowledge of the absorption spectra for atmospheric absorbers. Absorption spectra of ozone at different temperatures have been measured in the laboratory to quantify the absorption at stratospheric temperatures and to determine how the absorption depends on temperature [e.g., Bass and Paur,

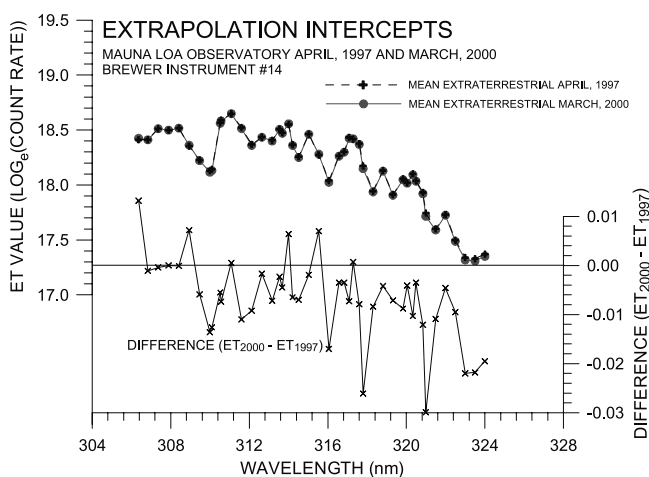


**Figure 5.** Average extraterrestrial spectra measured in April, 1997 and March, 2000 with the difference for the two calibration periods shown using the expanded scale on the right.

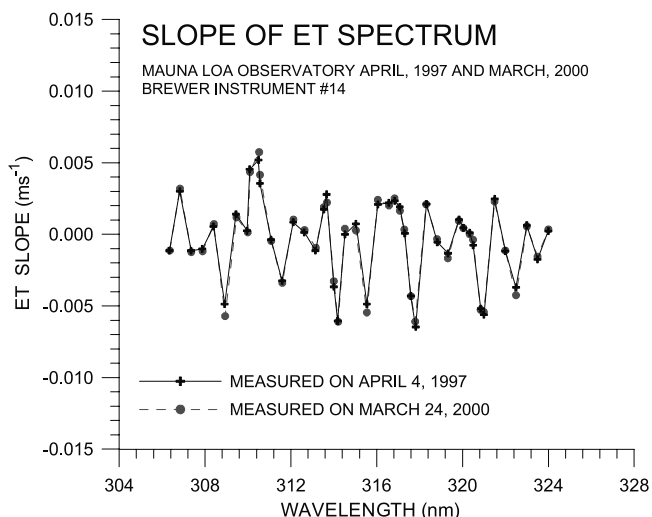


**Figure 6.** Slope of extraterrestrial spectrum measured at MLO in April, 1997 and March, 2000. The slopes are based on a second order polynomial ( $a_i + b_i * ms + c_i * ms^2$ ) fit to an over-sampled data set measured between  $\pm 10$  micrometer steps (ms) about each of the ( $i = 1$  to 45) wavelength settings. The values of  $b_i$  ( $= \Delta \log(I_o(\lambda_i) / \Delta ms)$ ) are shown here.

1985; Molina and Molina, 1986; Brion et al., 1993; Burrows et al., 1999]. Figure 8 shows the Bass and Paur [1985] (hereinafter referred to as BP) absorption spectra smoothed to the resolution of the Brewer instrument at six different temperatures ( $-70^\circ\text{C}$ ,  $-55^\circ\text{C}$ ,  $-45^\circ\text{C}$ ,  $-30^\circ\text{C}$ ,  $0^\circ\text{C}$  and  $25^\circ\text{C}$ ). The smoothing includes the convolution of the absorption spectra with the Brewer instrument slit functions (FWHI resolution of  $\sim 0.6$  nm) and the 0.15 nm resolved ET solar spectrum measured on the ATLAS-3 SUSIM Space Shuttle mission [VanHoosier, 1996]. The

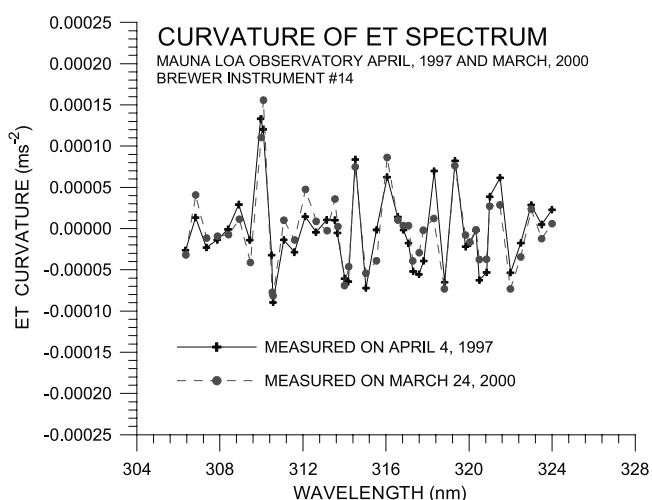


**Figure 7.** Curvature of extraterrestrial spectrum measured at MLO in April, 1997 and March, 2000. The curvatures are based on a second order polynomial ( $a_i + b_i * ms + c_i * ms^2$ ) fit to an over-sampled data set measured between  $\pm 10$  micrometer steps (ms) about each of the 45 wavelength settings. The values of  $c_i$  are shown here.

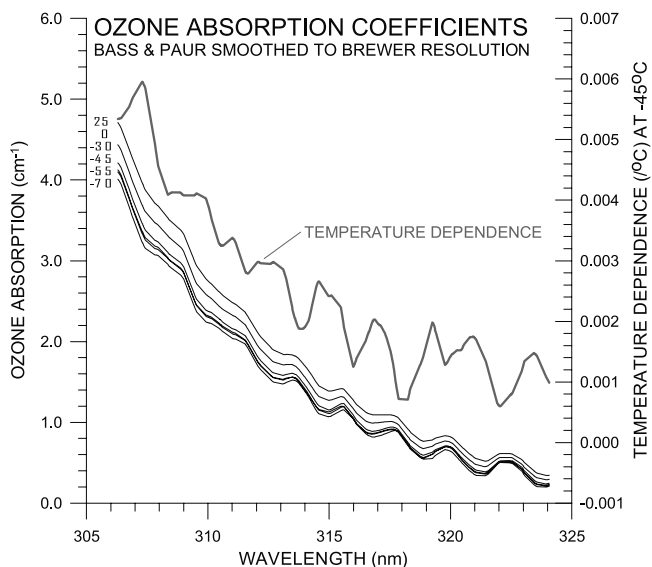


**Figure 8.** Ozone absorption coefficients at 6 temperatures as measured by Bass and Paur [1985] and smoothed to the resolution of Brewer instrument 14. The smoothing includes the weight of the extraterrestrial solar spectrum as measured by the Atlas-3 SUSIM Space Shuttle instrument [VanHoosier, 1996]. The temperature dependence of ozone absorption at  $-45^\circ\text{C}$  is also shown as determined from the slope of a quadratic fit to the five lowest temperatures.

45 smoothed absorption cross sections are given by  $\Sigma \alpha(\lambda) * S(\lambda) * ET(\lambda) / \Sigma S(\lambda) * ET(\lambda)$ , where  $\alpha(\lambda)$  are the BP absorption values,  $S(\lambda)$  are the 45 Brewer slit functions (Table 1) and  $ET(\lambda)$  is the ET solar spectrum. It is necessary to use the solar spectrum in the convolution process since different values ( $\sim 1\%$ ) are derived if a slowly varying smooth spectral source of radiation (i.e., a lamp) is used. Figure 8 also shows the temperature dependence spectrum derived from the slope (at  $-45^\circ\text{C}$ ) of a quadratic fit to the spectra using the 5 lowest temperatures. The ozone absorption coefficient values ( $\alpha(\lambda_i)$ ) and the temperature dependence values ( $\Delta \alpha(\lambda_i) / \Delta T$ ) at  $-45^\circ\text{C}$  are used as independent vectors of the DOAS analysis to determine the amount of total ozone (temperature independent) and the “effective” temperature of the ozone layer.

[22] A shift in wavelength setting ( $\delta ms$ ) for a measured spectrum affects the ozone absorption spectrum and the temperature dependence spectrum. In order to account for a wavelength shift it is necessary to adjust these spectra accordingly. This is done with knowledge of the slopes and curvatures of the ozone absorption and the slopes of the temperature dependence values as a function of micrometer steps around the 45 reference settings. These slopes and curvatures with respect to micrometer step values were determined by fitting polynomials to smoothed BP absorption values within  $\pm 10$  micrometer steps of the reference values.

[23] Figure 9 shows the average slopes of the ET extrapolations for the two calibration periods at all 45 wavelengths. The BP ozone absorption values at  $-45^\circ\text{C}$  smoothed to the resolution of the Brewer instrument are also shown. Comparison of the wavelength dependent

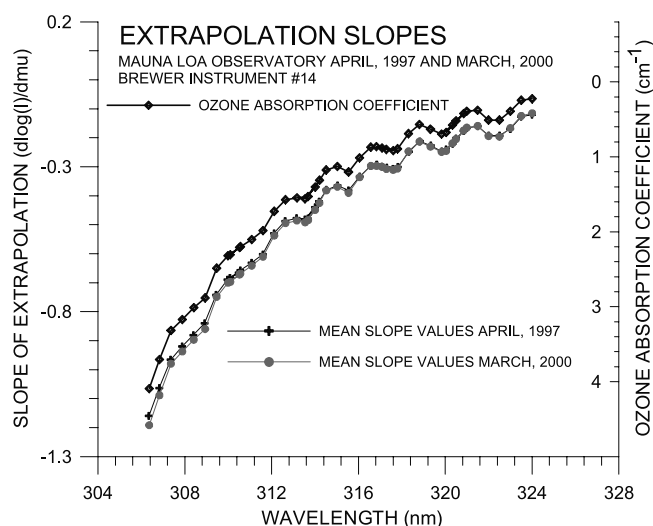


**Figure 9.** Mean values of the slopes of the Langley plots for the two MLO calibration periods compared with the BP ozone absorption spectrum smoothed to the Brewer resolution.

features of the average slopes with those of the ozone absorption spectrum illustrate that ozone is the main cause for atmospheric attenuation during the calibration periods. It was found that the best fit for the observed slopes was obtained when the BP spectra are shifted by +0.016 nm. This implied difference in wavelength may be due, in part, to the fact that the BP measurements were made in the laboratory using a spectrally smooth lamp source and the absorption values measured here used the highly structured solar spectrum as a light source.

[24] It should be noted that the method of derivation of ozone absorption coefficients used here differs considerably from that of determining the values used for the normal Brewer ozone measurements with the five operational wavelengths [Kerr *et al.*, 1985, 1988]. The operational method uses the BP absorption spectrum at  $-45^{\circ}\text{C}$  and not the spectrum obtained by fitting spectra measured at several temperatures, as is done here. The operational method does not shift the BP spectrum by +0.016 nm. Also the operational method assumes a spectrally flat light source and not the highly structured solar spectrum as the source.

Values of the absorption coefficients at the five wavelengths using the operational method (labeled “Operational”) and the method used here (labeled “Calculated”) are shown in Table 2. The weighted coefficient values for the Brewer ozone algorithm are also given. Comparison of the values determined by the two methods indicate that the differences are generally less than  $\pm 1\%$ .

## 5. Group-Scan Data Analysis Technique

[25] The group-scan DOAS analysis technique is based on equation (2). However, in practice, equation (2) must be augmented to account for the additional considerations which have been previously discussed. These considerations include variations of atmospheric conditions during the course of the scan, a possible wavelength shift between a measured scan and the reference, the fact that ozone absorption is temperature dependent, and the fact that other absorbers (primarily sulfur dioxide ( $\text{SO}_2$ )) may be present. In addition, it is assumed that the absolute responsivity of the instrument remains constant after appropriate corrections are made (temperature, neutral density filters, etc.).

[26] Analysis of a group-scan measurement is done by an iterative least square fitting procedure using the following set of 45 equations ( $i = 1$  to 45) based on equation (2) and denoting  $I_o(\lambda_i)$  by  $I_{oi}$ ;  $I(\lambda_i)$  by  $I_i$ ;  $\alpha(\lambda_i)$  by  $\alpha_i$ ;  $\beta(\lambda_i)$  by  $\beta_i$ .

$$\log(I_{oi}/I_i) - \beta_i m = A_g + B \frac{(I_i - 315 \text{ nm})}{315 \text{ nm}} + C \frac{\log(I_{oi})}{\text{ms}} + D a_i + E \frac{\Delta \alpha_i}{\Delta T} + F \alpha'_i + \epsilon_i \quad (3)$$

where  $g$  is the group number between 1 and 9;  $A_g$  are 9 attenuation offset values (one for each group) and are equivalent to the 9 different values of  $\tau_a$  at 315 nm that were present at the time of respective group samples;  $B$  is the linear wavelength dependence of  $\tau_a(315 \text{ nm})$ ;  $C$  is the number of micrometer steps ( $\delta\text{ms}$ ) between the reference scan ( $\log(I_{oi})$ , Figure 5) and the measured scan ( $\log(I_i)$ );  $\Delta \log(I_{oi})/\Delta \text{ms}$  are local slopes of the reference scan (Figure 6) with respect to  $\text{ms}$ ;  $D$  is ozone absorption in the path;  $\alpha_i$  are the ozone absorption coefficients at  $-45^{\circ}\text{C}$ ;  $E$  is the amount of ozone in the path times the temperature departure from  $-45^{\circ}\text{C}$ ;  $\Delta \alpha_i/\Delta T$  are the ozone temperature dependence values at  $-45^{\circ}\text{C}$  (Figure 8);  $F$  is the amount of  $\text{SO}_2$  in

**Table 2.** Operational, Calculated and Revised (From MLO Calibrations) Ozone Absorption Coefficients and Calculated and Revised (From 1998–1999 Toronto Data) Ozone Temperature Dependence Coefficients for the Normal Operational Wavelengths of Brewer Instrument 14

Wavelength, nm	Ozone Absorption Coefficients, $\text{cm}^{-1}$ at STP			$\text{O}_3$ Temperature Dependence, $\text{cm}^{-1}/^{\circ}\text{C}$	
	Operational	Calculated	Revised (MLO)	Calculated	Revised (Toronto)
306.360	4.0724	4.1037	4.0762	0.00535	0.00689
310.096	2.3113	2.3099	2.3047	0.00379	0.00398
313.541	1.5549	1.5637	1.5669	0.00212	0.00208
316.833	0.8637	0.8634	0.8637	0.00203	0.00229
320.040	0.6733	0.6782	0.6802	0.00145	0.00121
Normal Brewer ozone algorithm	0.7783	0.7815	0.7775	0.00073 (.094%/ $^{\circ}\text{C}$ )	-0.00004 (-.005%/ $^{\circ}\text{C}$ )

the path;  $\alpha_i$ ' are SO<sub>2</sub> absorption coefficients;  $\varepsilon_i$  are residual values at the 45 data points. The 14 unknown values (9A<sub>g</sub>'s, B, C, D, E and F) are solved by a multilinear least squares fit that minimizes the rms of  $\varepsilon_i$ . It should be noted that if the instrument responsivity does not remain constant (as assumed), then the effect would show up primarily as an error in the aerosol measurement. The most likely changes of instrument sensitivity (for example the transmission of the neutral density filters (Figure 1) or the temperature dependence (Figure 2)) would be one that is wavelength independent, thereby affecting the 9 A terms equally, and/or one that has near linear wavelength dependence, thereby affecting the B term.

[27] Results from the first iteration include the determination of wavelength shift, C (=  $\delta$ ms), and the amount of ozone in the path, D, from the least squares fit of (3) above. Once the wavelength shift is determined, the values of  $\log(I_{oi})$  and  $\Delta\log(I_{oi})/\Delta S$  are adjusted using the local slope (Figure 6) and curvature (Figure 7) values of the  $\log(I_{io})$  spectrum. The values of  $\alpha_i$  and  $\Delta\alpha_i/\Delta T$  are adjusted using their known dependencies on micrometer step number. The values of  $\alpha_i$  are also adjusted for non-linear absorption which results from strong gradients of the ozone absorption across the slit passbands and depends on the amount of ozone in the path [Vanier and Wardle, 1969; Gröbner and Kerr, 2001]. The regression using (3) is then repeated using the adjusted values to yield 14 new coefficient values. A stable solution is found when the new wavelength shift becomes negligibly small ( $|\delta$ ms| < 0.1 step), usually after one or two iterations. Spectra that are made under cloudy conditions generally do not converge to a solution after 3 iterations and are discarded.

[28] Values of atmospheric variables are determined from the 14 coefficients of the final iteration. The combined optical depth of aerosols ( $\tau_a(\lambda)$ , equation (2)) and thin clouds ( $\tau_{ci}(\lambda)$ ) at 315 nm is given by the mean value of the 9 A<sub>g</sub>'s ( $\bar{A}$ ) divided by the slant path through the aerosols or cloud ( $\sim m$  in equation (2) for  $m < 3$ ). Values for the wavelength dependence of aerosol optical depth is given by B. It should be noted that the Angstrom wavelength exponent [Angstrom, 1929] is approximated by  $-B/\bar{A}$ . Values for total ozone (D/ $\mu$ ), mean ozone temperature (E/D), and column SO<sub>2</sub> (F/m) are also determined.

[29] There are two indicators of the quality of the measurement that can be used as selection criteria. The first is the standard deviation of the nine offset values (A<sub>g</sub> values in equation (3)) that can be used to quantify the stability of atmospheric conditions during the scan. This group-to-group standard deviation will hereafter be referred to as the atmospheric variability indicator (AVI). The second indicator is the rms residual value which is used to estimate measurement uncertainty. Residual values ( $\varepsilon_i$  in (3)) should ideally be randomly distributed from wavelength-to-wavelength and from one scan to another. For a typical scan the maximum number of photons counted is set, by the neutral density filters, so that the peak value is usually of the order of 1–2 times 10<sup>6</sup>. The minimum number of photons counted in a particular scan (at 306.3 nm) ranges from 30% of the maximum (near 317 nm) when ozone in the path ( $\mu X$  in (3)) is relatively small to less than 5% of the maximum when  $\mu X$  is large. Therefore the random residual values estimated from Poisson counting statistics are

expected to be about  $\pm(0.001$  to  $0.002)$  at low  $\mu X$  and increase slightly as  $\mu X$  increases. In practice, however, there are often larger systematic departures due to causes such as changes in spectral characteristics of the instrument or incorrect absorption coefficients. Any systematic behavior of the residuals that shows up after the first pass analysis of the data set can be used to identify and correct problems for subsequent passes.

[30] Uncertainty estimates for the 14 derived quantities (unknowns) in equation (3) can be determined from the matrix (14 by 45 elements) of coefficients and the statistics of the observation errors. Assuming that the observation errors at the different wavelengths are random, uncorrelated of equal variance, as is implicit in the solution scheme, the uncertainties in the derived quantities are proportional to the rms residual. Standard uncertainty values so obtained, given the typical rms residual of 0.001, are as follows: for the 9 offsets (A's), 0.001; for the wavelength dependence term (B), 0.033; for the step number shift (C), 0.06 steps; for total ozone (D/ $\mu$ ), 1.0/ $\mu$  DU; for ozone temperature (E/D), 0.4/ $\mu X^\circ C$ ; and for SO<sub>2</sub> (F/m), 0.16/m DU.

[31] A minor effect which influences the measurement of direct radiation passing through the atmosphere (equation (2)) is the contribution of scattered radiation (either Rayleigh, aerosol or thin clouds) from within the field of view around the solar disk. This scattered radiation is added to the measured signal and therefore leads to an underestimation of the optical depth,  $\tau(\lambda)$ . Model calculations indicate that the ratio of additional Rayleigh scattered radiation to the transmitted radiation is approximately equal to  $0.00027 * \beta(\lambda) * m$  for the field of view of the Brewer instrument (nominally 3 solar diameters) for measurements made at 1 atmospheric pressure. This ratio is not dependent on ozone absorption, primarily due to the fact that the forward scattered radiation follows the same path through the ozone as the transmitted radiation. Although the Rayleigh scattering contribution is not particularly significant (<0.1% for  $m < 3$ ), corrections were made for this effect in the results reported here. Failure to correct for the Rayleigh scattering component would result in an underestimation of the A<sub>g</sub> (and  $\bar{A}$ ) terms in equation (3) by about 0.00027 (at  $\lambda = 315$  nm) at a pressure of 1 atmosphere. The effect on the wavelength dependent term, B in equation (3), is negligible.

[32] Estimating the contribution of scattered radiation from aerosols and thin clouds in the field of view around the Sun is more complicated. For the case of aerosols,  $\tau_a(\lambda)$  is divided into scattering and absorbing components ( $\tau_a(\lambda) = \tau_{sct}(\lambda) + \tau_{abs}(\lambda)$ ; e.g., Eck et al. [1999]). In general the ratio of scattered to transmitted radiation increases with the scattering component of the optical depth times the slant path ( $\tau_{sct}(\lambda) * s$ ). However, the ratio depends on the size, shape and absorption characteristics of the aerosol or cloud particles. There is more forward scattering, and thus more scattered radiation near the Sun with larger particle size [Kinne et al., 1997]. The overall consequences of the scattered radiation from around the Sun are to underestimate the optical depth ( $\bar{A}$ ) and, to a lesser extent, affect the linear dependence term (B in equation (3)) since the scattering and absorption characteristics of aerosol and cloud particles are smooth monotonic functions of wavelength. Again, the absorption from ozone and other atmospheric absorbers are minimally affected since the path of forward scattered

radiation through the atmosphere is virtually the same as that of the transmitted radiation.

## 6. Results

### 6.1. Mauna Loa Calibration Periods

[33] The spectra measured at MLO and used for calculating the instrumental ET spectrum were processed using the group-scan analysis technique with the BP absorption coefficients and temperature dependencies at  $-45^{\circ}\text{C}$  (from Figure 8). The performance of the group-scan method was initially assessed by examining the magnitude and behavior of the residuals. The rms residual values from the first pass of the MLO data for the March–April, 2000 calibration period are shown in Figure 10a. These residual values identified as initial pass are significantly larger than the expected value of  $\sim 0.001$ . When these first pass residual values are plotted as a function of air mass value (Figure 10b) significant air mass dependence is clearly seen.

[34] Figure 11 shows the residual spectra for several scans throughout the day on March 24, 2000, showing the presence of systematic wavelength-to-wavelength features that generally increase with increasing air mass. The systematic dependence is further illustrated in Figure 12 where the residual values at three wavelengths for all data from March 23–31, 2000 are plotted as functions of air mass times column ozone amount. The best fit linear regression of these plots (as well as those not shown for the other 42 wavelengths) all pass within a few units of 0.0001 (hundredths of a percent), indicating the precision with which the ET spectrum was measured. For all wavelengths the rms scatter ( $1\sigma$ ) of the data points about the best fit is approximately 0.001 and increases slightly with shorter wavelengths.

[35] The linear increase of the residuals with the amount of ozone in the path is a clear indication that there are small ( $<1\%$ ) relative differences between ozone absorption values measured in the laboratory and those measured by the absorption of solar radiation passing through atmospheric ozone. These differences arise from the fact that the BP absorption spectrum measured in the laboratory using a lamp as a light source at a FWHI resolution of  $\sim 0.025$  nm and smoothed to the Brewer resolution does not reproduce exactly the absorption observed in the atmosphere using a Brewer instrument at  $\sim 0.6$  nm resolution and the Sun as a source. Also, the ozone in the atmosphere is not all at the same temperature. The resulting absorption spectrum seen in the atmospheric situation is a sum of many temperature dependent spectra weighted by the fractional amount of ozone at each temperature.

[36] The slopes of the best linear fits of the residuals plotted against the amount of ozone in the path (as illustrated in Figure 12) are the corrections required to the ozone absorption coefficient values. Figure 13 shows the required corrections of the absorption coefficient values for the two calibration periods of April, 1997 and March 2000. The corrected values at the five operational Brewer wavelengths are shown in Table 2 (labeled “Revised”). For most of the wavelengths these corrections are less than  $\pm 1\%$ . There is reasonably good agreement between the corrections required for the two calibration periods.

[37] Another pass of the group-scan analysis was carried out using the ozone absorption spectrum corrected by the

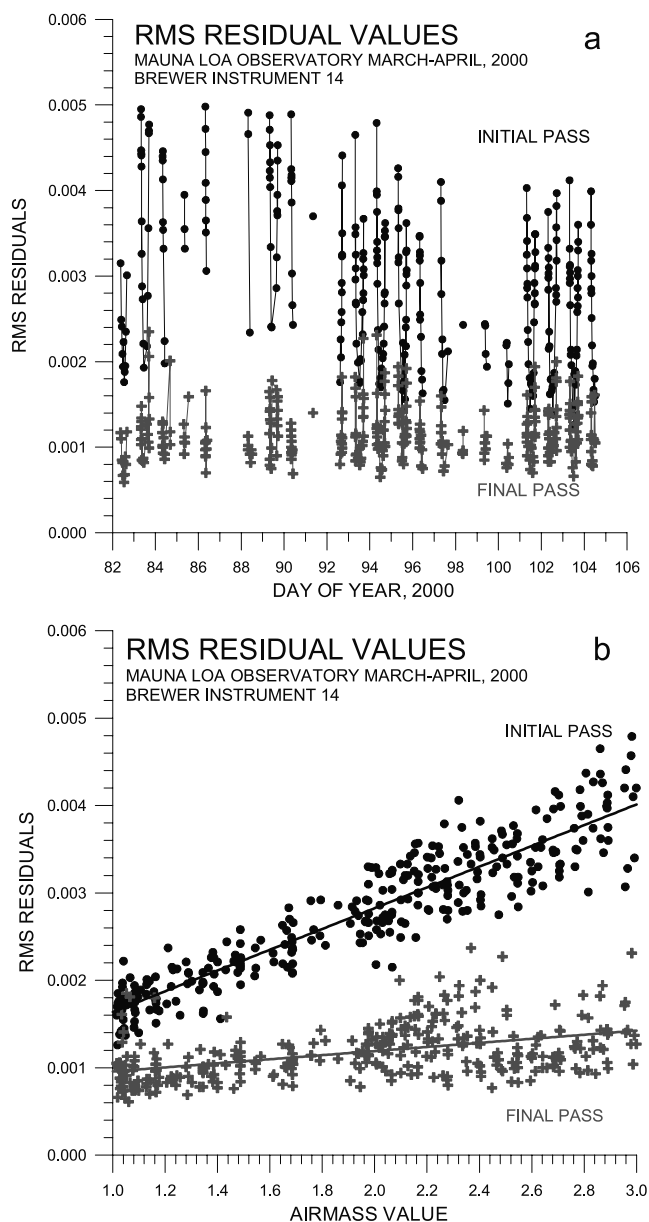


**Figure 10.** Daily record (a) and air mass dependence (b) of rms residual values for the March–April, 2000 MLO calibration. The relatively large initial pass residuals that increase with air mass are due to improper values of ozone absorption coefficients, which, when corrected, result in significantly reduced final pass residuals and air mass dependence.

values shown in Figure 13. The rms residual values remaining after this pass are significantly reduced and are shown in Figures 10a and 10b for comparison with the residuals after the initial pass. After the final pass a significant fraction of the spectra have rms residual values less than 0.001 (the expected value) and nearly all rms residuals are less than 0.002. The air mass dependence of the rms residuals is also significantly reduced (Figure 10b). The slight remaining air mass dependence is explained by the fact that the signal (photon count) gradient of the scan increases with larger air mass values. Figure 14 shows the residual values after the

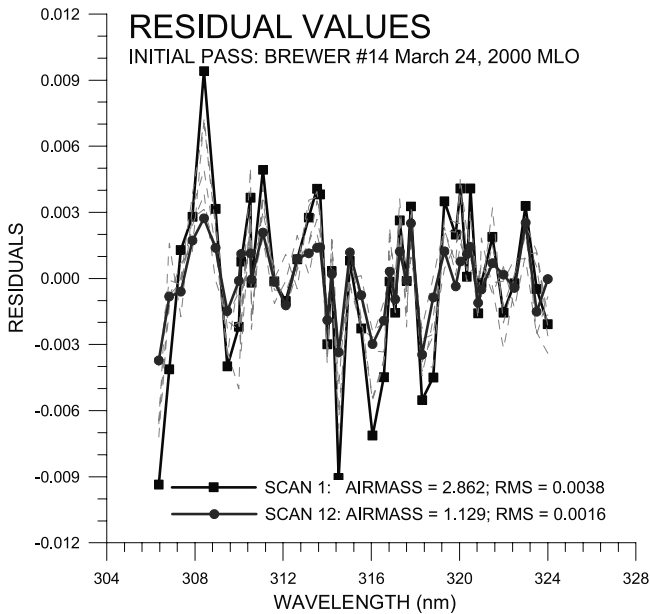


**Figure 11.** Examples of initial pass residuals from spectra observed on March 24, 2000. The rms residuals and wavelength dependent features generally increase with airmass.

second pass for the same spectra on March 24, 2000 shown in Figure 11. The systematic wavelength-to-wavelength and scan-to-scan variations are no longer present.

[38] Figure 15 shows the record of wavelength settings relative to the reference for all scans taken during the calibration in March–April, 2000. This measurement indicates the wavelength stability of the instrument. Wavelength

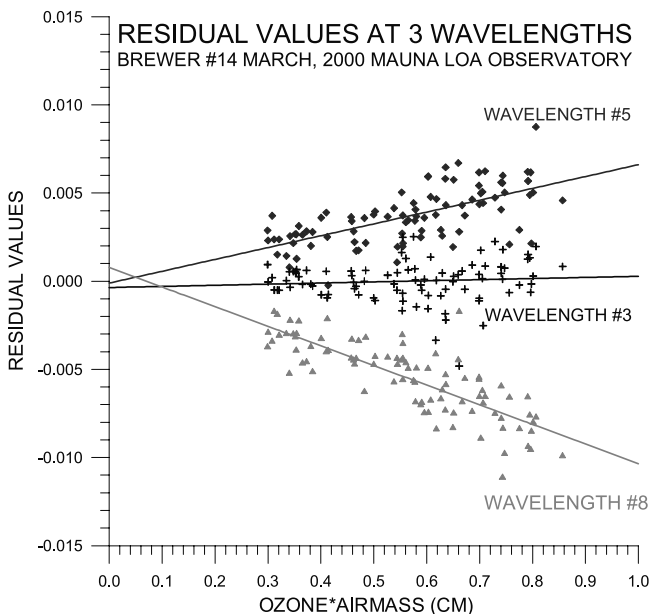


**Figure 12.** Dependence of residual values on the amount of ozone in the atmospheric path at selected wavelengths. The slopes of the lines fit to the residual values are corrections that are required to the ozone absorption coefficients.

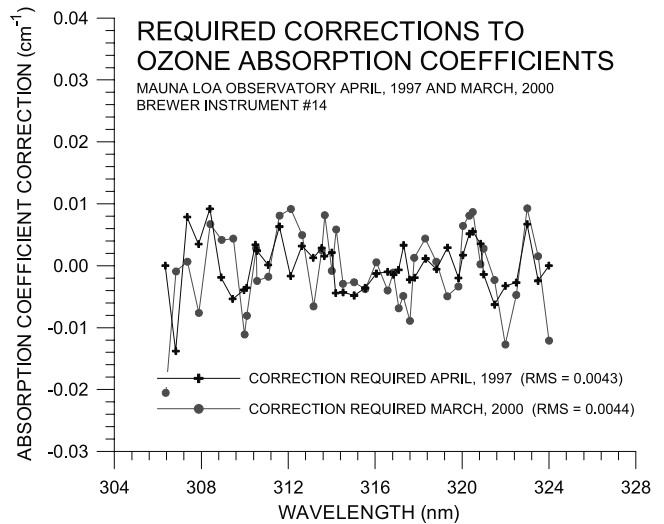


**Figure 13.** Observed corrections required for ozone absorption coefficients at all 45 wavelengths for the two MLO calibration periods in April, 1997 and March, 2000. In general the corrections are less than  $\pm 1\%$  of the coefficient values.

settings using an emission line as a light source are typically measured to within a tenth of a micrometer step (1 micrometer step  $\sim 7.0 \text{ pm} = 0.007 \text{ nm}$ ), a value well within the one step positioning capability of the instrument [Gröbner *et al.*, 1998]. It was found here that wavelength settings using the solar spectrum as a reference are determined to approximately the same accuracy, in good agreement with that expected from the error estimated from the residual values. Variations by as much as 3 micrometer steps were seen during the first part of the MLO 2000 calibration, mainly as

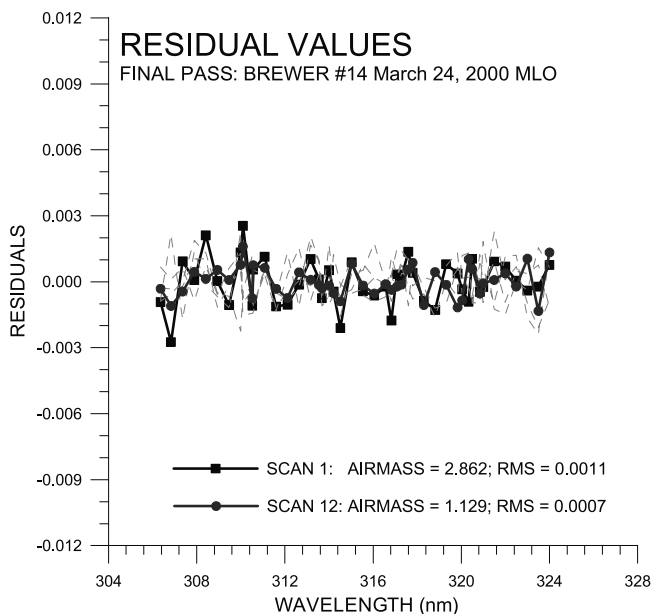


**Figure 14.** Final pass residuals from spectra observed on March 24, 2000, as in Figure 11. There is little wavelength-to-wavelength and air mass dependence of the final pass residuals.

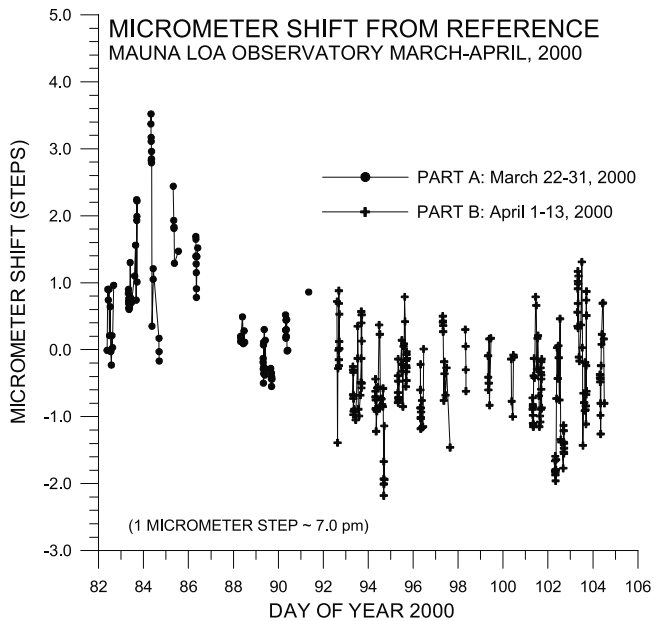


**Figure 15.** Wavelength shift of observed spectra relative to reference for the MLO calibration in March–April, 2000.

a result of a misalignment of the zenith prism with the mercury calibration lamp. This problem was fixed for the second part of the calibration period and departures from the reference were reduced.

[39] The record of total ozone values for the MLO calibration period in 2000 is shown in Figure 16. There were some small ozone variations throughout most days showing daily standard deviations of about  $\pm 1$  or  $\pm 2$  DU. Some days with very stable ozone (e.g., Day 92–April 1) had standard deviations of about  $\pm 0.5$  DU for 12 observations spread over 2 hours, the accuracy expected from observed residual values.

[40] Figure 17 shows the record of column  $\text{SO}_2$  for the period. The standard deviation of  $\text{SO}_2$  for the period was observed to be about  $\pm 0.13$  DU, a value larger than that expected from the residual values. There is a possibility that the larger than expected variability could be due to trace amounts of volcanic  $\text{SO}_2$  that sometimes pass over the site.

[41] Aerosol optical depth values ( $\tau_a(315 \text{ nm})$ ) and their standard deviations (given by  $\text{AVI}/\mu$  and indicated by error bars) are shown in Figure 18. It should be noted that the AVI values are generally in good agreement with expected random errors ( $\sim \pm 0.001$ ) when the aerosol optical depth is small ( $\sim 0.05$ ). When optical depth values are larger a significant increase in the AVI is observed indicating real atmospheric variability. Comparison of the AVI values with the final pass residual values (from Figure 10) demonstrates the effectiveness of the group-scan method. Figure 19 shows the ratio of the AVI to residual values. The minimum value of the ratio for most of the measurements is around 1, the value expected from Poisson noise with a stable atmosphere with sample-to-sample variability  $\sim \pm 0.1\%$ . However, about 10% of the ratios are larger than 5 indicating that variability due to changing atmospheric conditions during the course of the scan is about 5 times that expected from Poisson noise. It is also interesting to note that useful scan data are obtained when the AVI is more than 10 times the

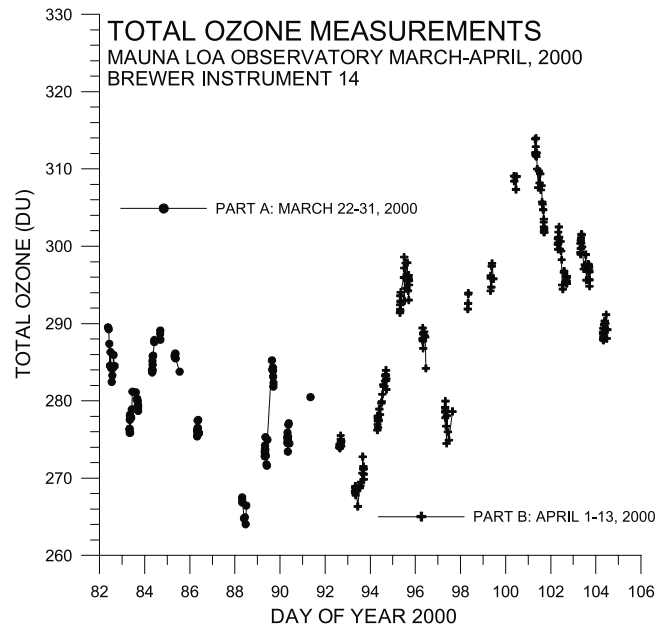


**Figure 16.** Total ozone measured during the March–April, 2000 MLO calibration. The point-to-point variations are generally less than 1 DU and agree with the uncertainty expected from Poisson noise.

residual value. Spectra taken under these variable atmospheric conditions ( $> \pm 1\%$  sample-to-sample variability) using a slower conventional scanning technique would likely be unusable.

[42] Daily average values of effective column ozone temperature and their standard deviations are shown in

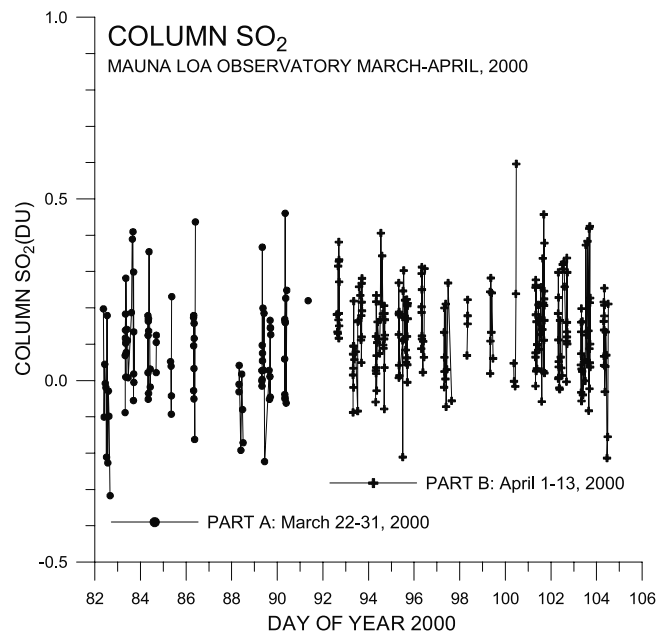


**Figure 17.** Column  $\text{SO}_2$  measurements for the March–April, 2000 MLO calibration period. The standard deviation of all  $\text{SO}_2$  measurements is  $\pm 0.13$  DU. The two occasions when  $\text{SO}_2$  was above 0.5 DU may be an indication of volcanic  $\text{SO}_2$ , which is sometimes present at the site.

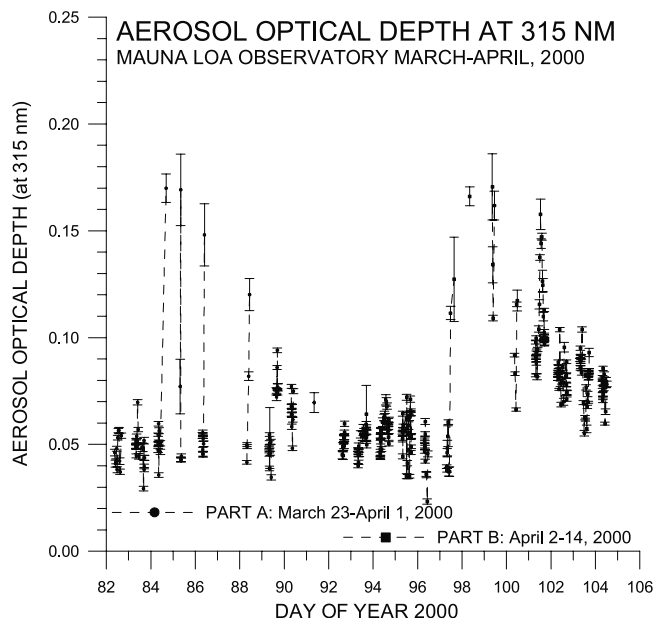


**Figure 18.** Measurements of the aerosol optical depth ( $\tau_a(315 \text{ nm})$ ) during the March–April, 2000 MLO calibration period. Error bars indicate the standard deviation of the offset terms for the nine groups. When optical depth values are small the standard deviations are in good agreement with the uncertainty expected from Poisson noise. Larger standard deviations that occur when the optical depth values are larger indicate real atmospheric variability during the course of the scan.

Figure 20. These remotely measured values of ozone temperature ( $-43^\circ\text{C}$  to  $-45^\circ\text{C}$ ) are in good agreement with effective ozone temperatures measured at this time of year by ozonesondes flown from Hilo, Hawaii. The solid smooth line in Figure 20 is the smoothed average of the effective ozone temperatures measured by ozonesonde flights between 1982 and 1997. The two crosses are the effective ozone temperature determined from ozonesonde flights on March 29 and April 12, 2000. The observed daily standard deviation of about  $\pm 0.8^\circ\text{C}$  is in good agreement with estimated random errors.

## 6.2. Toronto

[43] Brewer instrument 14 is one of the three members of the triad reference for Brewer instruments [Kerr *et al.*, 1985, 1998] and normally takes routine measurements at Toronto. Measurements using the new group-scan technique have been made with this instrument at Toronto since November, 1996. During the period between November, 1996 and June 2001 30790 group scans were attempted. Results of the first part of the 1997 MLO calibration (March, 1997) were used to process Toronto data from November 1996 to March 1997 and results from the second part (April, 1997) were used for Toronto data from April to September, 1997. Results from the first part of the 2000 MLO calibration (March, 2000) were used to process Toronto data between September, 1997 and March, 2000 and results from the second part (April, 2000) used for data after April, 2000.

[44] Figure 21 shows the record of rms residual values measured at Toronto between November, 1996 and June,

2001. On the initial pass data are accepted if the rms residual value is less than 0.008 and the standard deviation of optical depth ( $\text{AVI}/\mu$ ) is less than 0.02. Of the 30790 scans attempted 7384 met these conditions in the initial pass. Values of the residuals after the initial pass are as much as 0.007 during some parts of the record. These values are considerably larger than those expected from random errors due to photon counting noise ( $\sim 0.001$  to  $0.002$ ) as discussed earlier and those seen at MLO (Figures 10a and 10b) after small changes ( $<1\%$ ) were applied to the ozone absorption spectrum (Figure 13). For the analysis of data at MLO it was not necessary to consider variations in the characteristics of the instrument which was quite stable over the relatively short time period of a few days. It is quite clear from Figure 21 that the stability of the instrument over longer time periods (a few years) must be considered in the analysis of the Toronto data record. There are several causes for the increased values of the residuals seen at some times during the record. Analysis of this record of the residuals can provide information regarding the absorption properties of atmospheric constituents (mainly ozone) as well as a diagnostic of the performance and stability of the instrument.

[45] The enhanced residual values ( $\sim 0.007$ ) between the beginning of 1998 and the middle of 1999 are due to a relatively constant residual spectrum that persisted throughout this period. The mean and standard deviation of all (2210) residual spectra between July, 1998 and June, 1999 are shown in Figure 22. The fact that the standard deviations

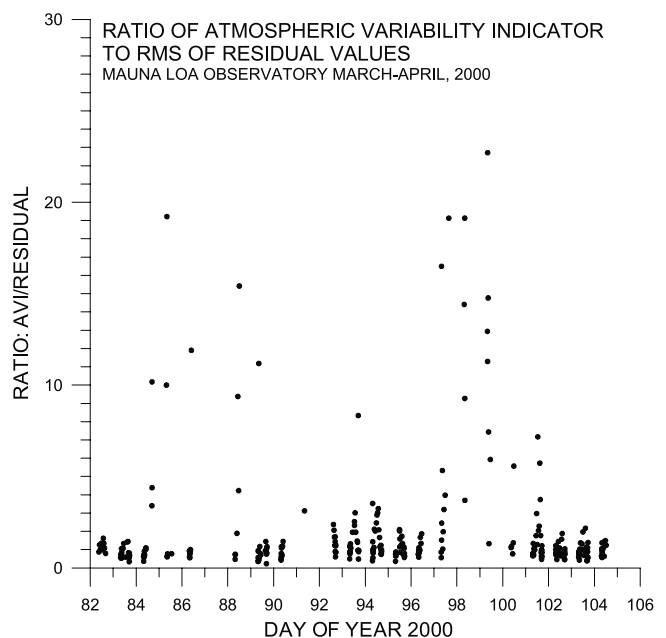


**Figure 19.** Ratio of the atmospheric variability indicator (AVI) to rms residual values for the group scans measured at MLO during the March–April, 2000 calibration. Values of about 1 for this ratio indicate a stable atmosphere with little variability ( $\sim \pm 0.1\%$ ) from sample-to-sample. Values greater than 10 indicate sample-to-sample variability of atmospheric conditions greater than  $\pm 1.0\%$ , conditions which would likely not yield usable spectra using a conventional slower scanning technique.

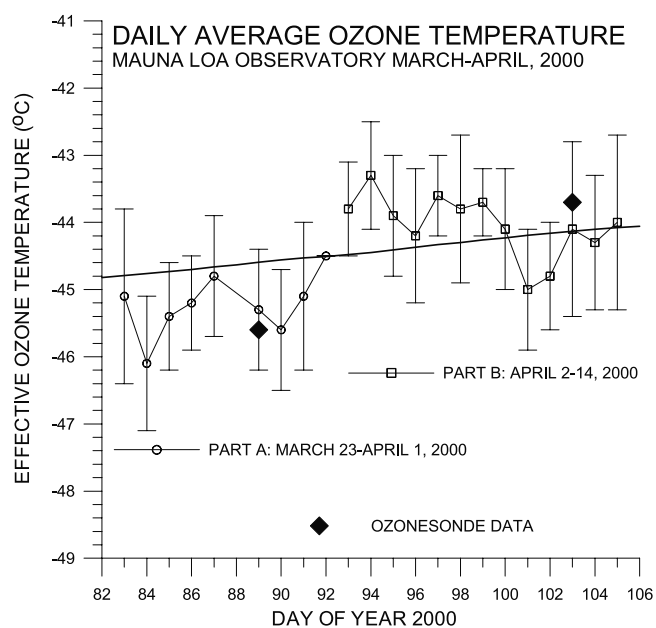


**Figure 20.** Daily average values of the effective temperature of column ozone. These values are in good agreement with ozone weighted temperatures measured by ozone sondes flown from Hilo, Hawaii at this time of year. The error bars indicate daily standard deviations and are in good agreement with expected uncertainties.

of the residuals are generally consistent with Poisson noise (between 0.001 and 0.002) indicates that the instrument was quite stable over this period. However, the average residual values vary by  $\pm 0.005$  from wavelength-to-wavelength and some values are as large as  $\sim \pm 0.01$ . It is apparent that the reference spectrum which should be used for the analysis during this period differs from the one that was used (measured at MLO in March, 2000). The differences are

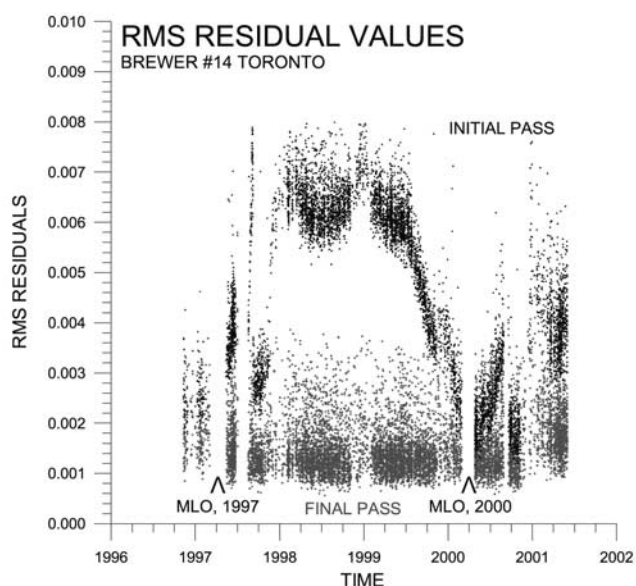


**Figure 21.** The initial and final rms residuals for the 4 year data record of direct sun group-scan measurements at Toronto. Calibration periods at MLO are indicated.

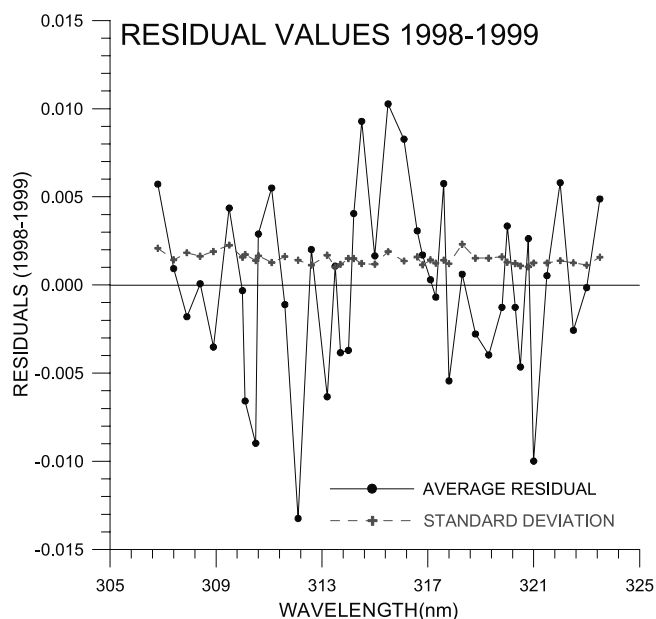


**Figure 22.** The wavelength-to-wavelength mean and standard deviation of all residual values between July, 1998 and June, 1999. These residuals are the result of instrumental changes that occurred between this period and the MLO calibration. The fact that the standard deviations show little wavelength dependence and are of the order expected from Poisson noise indicates that the instrument was relatively stable from July, 1999 to June, 1998.

due to small changes of instrumental optical characteristics (relative wavelength settings or slit resolutions) interacting with the highly structured solar spectrum. It is of interest to note that the residuals near the end of 1997 are similar to those at the beginning of 2000. This indicates that the optical configuration of the instrument shifted from one similar to that at MLO in late 1997 to the stable 1998–1999 configuration and then back to the MLO configuration in early 2000.

[46] The record of daily mean values for the effective ozone temperature from the analysis is shown over the 4 year period at Toronto in Figure 23a and as a function of day of year in Figure 23b. Ozone temperature varies from about  $-49^{\circ}\text{C}$  in winter to about  $-41^{\circ}\text{C}$  in summer. The typical standard deviation for a daily set of measurements is about  $0.8^{\circ}\text{C}$ .

[47] Further analysis of residual values was carried out over the one year period from July, 1998 to June, 1999. This allowed the determination of the dependence of residual values on ozone temperature over a complete annual cycle when the instrumental characteristics remained stable. It was found that the residuals at some wavelengths depend on ozone temperature, indicating that the temperature dependence values are not correct. A revised set of temperature dependence coefficients was determined from the slopes of the residual values plotted as a function of ozone in the path times ozone temperature departure from  $-45^{\circ}\text{C}$  (E in equation (3)). The revised spectrum and calculated (from Figure 8) spectra of temperature dependence values is shown in Figure 24 along with the MLO revised ozone absorption coefficients. In the case of the MLO revision of

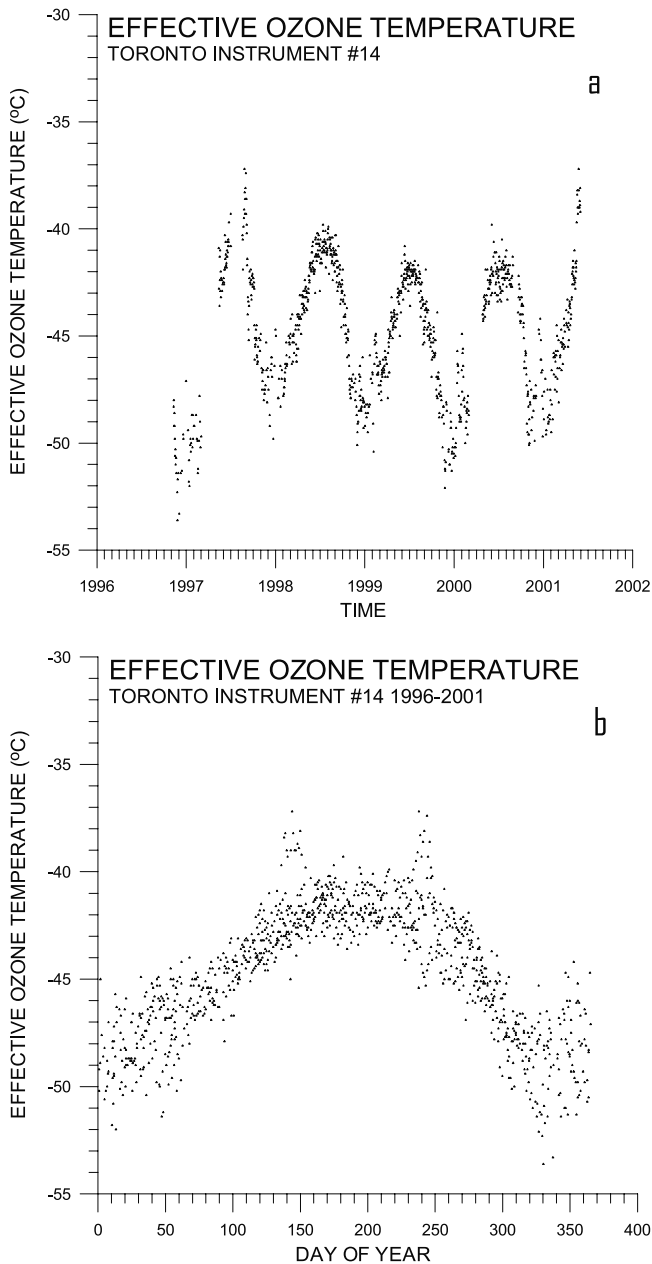


**Figure 23.** Record of effective ozone temperature measured at Toronto between 1996 and 2001 (a) and as a function of day of year (b).

the ozone absorption coefficients the changes are generally less than  $\pm 1\%$  (Figure 13). In the case of the temperature dependence there are large differences between the calculated and revised results. It is apparent from Figure 24 that the revised set of temperature dependence values show better alignment with the peaks and valleys of the absorption coefficients than do the calculated temperature dependence values. Figure 24 indicates the normal operational wavelengths for the Brewer instrument. The values of the calculated and revised sets of temperature dependence coefficients for these wavelengths are given in Table 2.

[48] The spectral data were reprocessed using the revised temperature dependence coefficients. Also the reference spectrum was adjusted as a function of time by adding the

average of several residual spectra taken within 10 days. The final pass of the data accepted 9941 of the 30970 spectra with rms residuals less than 0.0035 and no limit was set for the AVI values. The record of rms residual values after the final processing of the data is shown in Figure 21 and is generally consistent with values expected from Poisson counting noise.

[49] The record of total ozone measurements at Toronto over the period are shown in Figure 25. These ozone values are in good agreement (generally to within  $\pm 1\%$ ) with the Brewer reference triad [Kerr *et al.*, 1985]. A detailed comparison of results from this new measurement method will be included as part an evaluation of the long-term performance of the Brewer reference triad to be published in the near future.

[50] Figure 26 shows the record of the optical depth of aerosols and thin clouds over Toronto and Figure 27 shows the ratio of AVI values to residual values. The results shown in Figure 27 demonstrate how well the group-scan method works. Specifically the variability of the atmosphere from sample-to-sample is often more than 2 orders of magnitude greater than the rms residual values that result from the group-scan analysis. For the Toronto record about 40% of the spectra were made when atmospheric conditions were varying more than 10 times the group-scan residual values and about 60% were made with the AVI more than 5 times the residuals. Significantly noisier spectra would be measured under these observing conditions using conventional scanning techniques that are affected by changes in atmospheric conditions from sample-to-sample. The rms residual values would increase by roughly the ratios shown in Figure 27 as would the uncertainty estimates for the measured

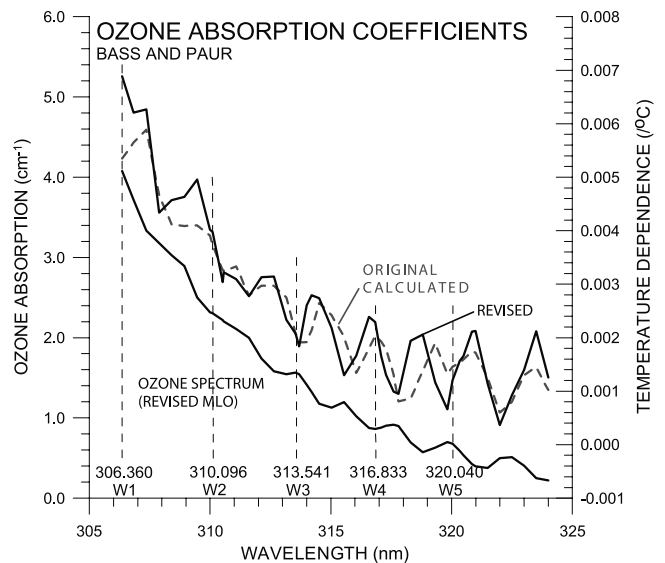


**Figure 24.** The revised and calculated (from Figure 8) spectra of temperature dependence values with the MLO revised ozone absorption coefficients. There are large differences between the calculated and revised results. The revised set of temperature dependence values show better alignment with the peaks and valleys of the absorption coefficients than do the original temperature dependence values. The normal operational wavelengths for the Brewer instrument are shown.

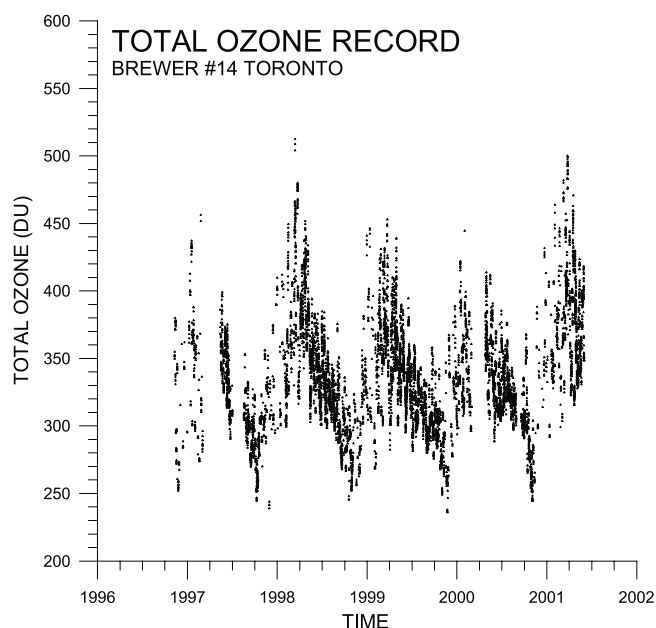


**Figure 25.** Total ozone measured at Toronto between 1996 and 2001 using the group-scan technique.

parameters rendering a significant fraction of the measurements ( $\sim 50\%$ ) not very usable.

[51] The AVI value could potentially be used as an indicator to determine whether the measured optical depth is due to aerosols or thin clouds. It is quite likely that aerosols would have lower temporal variability than thin clouds over the course of the scan.

## 7. Discussion

[52] In general, as the precision of a measurement increases, more uncertainties affecting the measurement

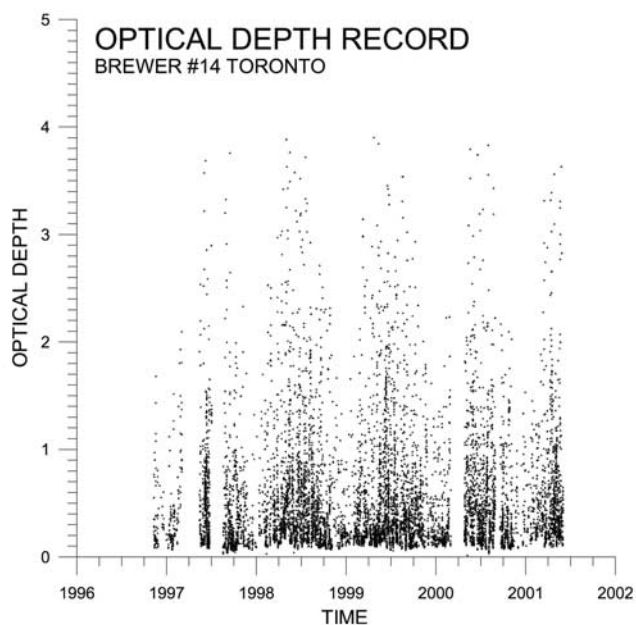


**Figure 26.** Record of aerosol optical depth ( $\tau_a(315 \text{ nm})$ ) measured at Toronto between 1996 and 2001.

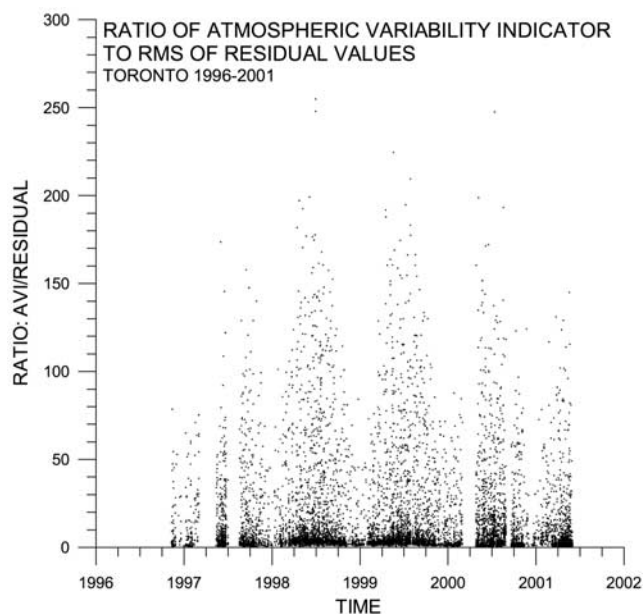


**Figure 27.** Record of the ratio of AVI to residual values, demonstrating how well the group-scan method works under atmospheric conditions that vary from sample-to-sample by more than  $\pm 50\%$ , more than 2 orders of magnitude more than the residuals.

must be considered and properly addressed. This study has presented results that are based on measurements made with precision of the order of  $\pm 0.1\%$ . It has been demonstrated that there are several factors that can potentially decrease this precision. It is important to know accurately and understand fully the optical characteristics of the particular instrument being used. Instrument stability is an important consideration, particularly over long time periods (a few years). Any small ( $< 1.0\%$ ) systematic changes in the measurements resulting from instrumental changes must be properly assessed and corrected. Accurate knowledge of the absorption spectra of atmospheric constituents is also essential.

[53] One important instrumental consideration is the effect of stray light. It was found essential to apply correction for stray light in the single monochromator (Brewer instrument 14) used in this study in order to achieve the required precision. This correction is made in the operational data analysis used to calculate UV spectra measured with single Brewer instruments, but is not, as yet, made in the operational calculation of ozone values. During the course of this study, the stray light scattering characteristics changed in the instrument. The spectrometer mirror was cleaned at MLO in April, 2000 (between part 1 and part 2 of the calibration segments) and significant improvement of stray light properties were measured. The question of long-term gradual changes in instrumental stray light should be considered. One method to avoid the stray light problem is to use a double monochromator in a study similar to this.

[54] This study has also shown that it is important to know values for ozone absorption coefficients and their temperature dependence very accurately. It is quite likely that

absorption spectra measured accurately in the laboratory will require some adjustment when applied to the situation where the absorption occurs in the atmosphere with the Sun as a light source. Slightly different results were obtained when absorption spectra of others [Brion *et al.*, 1993; Burrows *et al.*, 1999] were used. These differences are systematic and they originate from differences in the laboratory measured spectra. Ideally it would be desirable to use the same instrument to measure absorption spectra in the laboratory as the one used to take atmospheric measurements.

[55] Comparison of direct sun total ozone values measured by Dobson and Brewer instruments has consistently shown that there is a systematic annual difference between the two instrument types [Kerr *et al.*, 1988, 1989; Vanicek, 1998; Staehelin *et al.*, 1998; Köhler, 1999]. When compared with Brewer total ozone values, Dobson values are typically 1% to 3% higher in summer than they are in winter. Kerr *et al.* [1988] suggested that a possible cause could be the difference in temperature dependence for the sets of ozone absorption coefficients used by the Brewer and Dobson instruments. However, a large annual range in ozone temperature ( $\sim 20^\circ\text{C}$ ) would be required if the temperature dependence is  $+0.13\%/^\circ\text{C}$  for Dobson AD measurements and  $+0.07\%/^\circ\text{C}$  for Brewer measurements. (The value of  $+0.07\%/^\circ\text{C}$  given by Kerr *et al.* [1988] differs from the value of  $+0.094\%/^\circ\text{C}$  shown in Table 2 because the previous determination was from a quadratic fit to all 6 of the BP temperatures and the present study uses spectra at the 5 lowest BP temperatures). If the temperature sensitivity of the Brewer measurement is small ( $-0.005\%/^\circ\text{C}$ ), as suggested by this study, then the annual range of  $\sim 1\%$  Dobson/Brewer ratio seen in Toronto is easily explained by the  $8^\circ\text{C}$  range of ozone temperature (Figure 23b) and the  $+0.13\%/^\circ\text{C}$  temperature dependence of the Dobson measurements. Also, the good agreement in the shape of the annual temperature variation shown in Figure 23b and the shape of the annual Dobson/Brewer ratio shown in Figure 5 of Kerr *et al.* [1988] suggests that the temperature sensitivity of Dobson measurements is the main cause.

[56] Brewer instruments have accumulated a vast quantity of data using the operational 5 wavelength technique at many locations and for nearly 20 years at some sites. In principle it is possible to extract 5 pieces of information from 5 measurements. It may be possible to re-analyze the archived data to extract additional information such as aerosol optical depth and ozone temperature. Results of the analysis of the 4 year group-scan data set have demonstrated that instrumental effects (such as stray light and temperature response) must be carefully considered and absorption coefficients must be accurately known. It is planned to investigate the possibility of re-analyzing the Brewer data archives at some sites using information gained by this study.

[57] In addition to the direct sun measurements presented here, global irradiance and zenith sky spectra have also been measured with the same instrument using the group-scan sampling method over the same time period. These measurements have been made throughout the day from sunrise to sunset. During the middle part of the day, when the airmass value,  $\mu$ , is less than 3.5, the global and zenith sky irradiance observations are made sequentially within 3

minutes of the direct sun measurements. These spectra have been taken under conditions with a wide range of variables such as cloud cover, haze and albedo. Analysis of the global and zenith data sets have yet to be carried out. It is expected that by using the group-scan analysis technique on the global and zenith spectra the effects of changing conditions during the course of the scans will be removed as they were with the direct sun spectra. It is hoped that the analysis of clean (low noise) zenith sky and global irradiance spectra taken simultaneously with direct sun spectra under a wide range of conditions will contribute significantly to a better understanding of scattering and absorption processes that occur in the atmosphere that may lead to improved retrieval of total ozone, ozone profile (Umkehr) and ozone temperature under variable sky conditions.

## 8. Summary

[58] A new technique has been developed for carrying out spectral studies of atmospheric variables using the Brewer spectrophotometer. The technique includes a new method for sampling and analyzing ultraviolet spectra that essentially removes effects of varying atmospheric conditions during the course of the scan. It was demonstrated that spectral irradiance measurements can be made with a precision comparable with that expected from random Poisson noise ( $\sim \pm 0.1\%$ ). Spectra with these low uncertainties can be used to measure atmospheric variables accurately and identify instrumental problems with greater certainty provided effects of the order of  $\pm 0.1\%$  are carefully addressed. It was found necessary to measure accurately the wavelength settings and resolution of the instrument and to consider carefully instrumental effects such as temperature dependence, filter attenuation, dark count, dead time and stray light.

[59] Langley plots of direct sun irradiance measurements at wavelengths between 306 and 324 nm were made at MLO, Hawaii using a single Brewer monochromator (instrument 14). An extraterrestrial spectrum was measured that is in good agreement with other ground-based and satellite based values. This spectrum was used as a reference to process data measured at MLO and Toronto. Analysis of data measured with the clean and stable conditions at MLO demonstrated that the potential of the new scanning method is achieved.

[60] Results of measurements made at Toronto demonstrate that it is possible to obtain an "effective" temperature value for atmospheric ozone. These measurements suggest that the temperature dependence of ozone absorption has little effect on Brewer total ozone values and that the temperature dependence of the Dobson total ozone measurement likely explains most of the observed seasonal differences between Dobson and Brewer measurements.

[61] **Acknowledgments.** The author would like to thank those who made valuable contributions to this work. David Wardle and Tom McElroy provided many useful suggestions and comments regarding the instrumental and technical aspects of the new technique as well as the analysis and interpretation of the data. Vitali Fioletov provided input in processing the data. Chris McKlinden carried out model calculations of Rayleigh atmospheres. Two anonymous reviewers made constructive suggestions. Tom Grajnar provided significant assistance in maintaining, calibrating and operating the instrument both in Toronto as well as at Mauna Loa.

## References

- Angstrom, A., On the atmospheric transmission of Sun radiation and on dust in the air, *Geogr. Ann.*, 12, 130–159, 1929.
- Bais, A. F., Absolute spectral measurements of direct solar ultraviolet irradiance with a Brewer spectrophotometer, *Appl. Opt.*, 36, 5199–5204, 1997.
- Bass, A. M., and R. J. Paur. The ultraviolet cross-sections of ozone, I, The measurements, in *Atmospheric Ozone: Proceedings of the Quadrennial Ozone Symposium Held in Halkidiki, Greece, 3–7 September 1984*, edited by C. S. Zerefos and A. Ghazi, pp. 606–610, D. Reidel, Norwell, Mass., 1985.
- Bates, D. R., Rayleigh scattering by air, *Planet. Space Sci.*, 32, 785–790, 1984.
- Brion, J., A. Chakir, D. Daumont, J. Malicet, and C. Parisse, High-resolution laboratory absorption cross section of O<sub>3</sub>: Temperature effect, *Chem. Phys. Lett.*, 213, 610–612, 1993.
- Burrows, J. P., A. Richter, A. Dehn, B. Deters, S. Himmelmann, S. Voigt, and J. Orphal, Atmospheric remote sensing reference data from GOME, 2, Temperature dependent absorption cross sections of O<sub>3</sub> in the 231–794 nm range, *J. Quant. Spectrosc. Radiat. Transfer*, 61, 509–517, 1999.
- Carvalho, F., and D. Henriques, Use of the Brewer spectrophotometer for aerosol optical depth measurements in the UV region, *Adv. Space Res.*, 25, 997–1006, 2000.
- Dobson, G. M. B., Observers' handbook for the ozone spectrophotometer, *Ann. Int. Geophys. Year*, 5, part 1, 46–89, 1957.
- Eck, T. F., B. N. Holben, J. S. Reid, O. Dubovik, A. Smirnov, N. T. O'Neill, I. Slutsker, and S. Kinne, Wavelength dependence of the optical depth of biomass burning, urban, and desert dust aerosols, *J. Geophys. Res.*, 104, 31,333–31,349, 1999.
- Fioletov, V. E., J. B. Kerr, D. I. Wardle, E. Wu. Correction of stray light for the Brewer single monochromator, paper presented at Quadrennial Ozone Symposium, Natl. Space Dev. Agency of Japan, Sapporo, 2000.
- Gröbner, J., and J. B. Kerr, Ground-based determination of the spectral ultraviolet extraterrestrial solar irradiance: Providing a link between space-based and ground-based solar UV measurements, *J. Geophys. Res.*, 106, 7211–7217, 2001.
- Gröbner, J., D. I. Wardle, C. T. McElroy, and J. B. Kerr, Investigation of the wavelength accuracy of Brewer spectrophotometers, *Appl. Opt.*, 37, 8352–8360, 1998.
- Gröbner, J., R. Vergaz, V. E. Cachorro, D. V. Henriques, K. Lamb, A. Redondas, J. M. Vilaplana, and D. Rembges, Intercomparison of aerosol optical depth measurements in the UVB using Brewer spectrophotometers and a Li-Cor spectrophotometer, *Geophys. Res. Lett.*, 28, 1691–1694, 2001.
- Gustin, G. P., et al., Ozonometer M-124 (in Russian), *Tr. Gl. Geofiz. Obs. im. A.I. Voeikova*, 499, 60–67, 1985.
- Hofmann, D., et al., Intercomparison of UV/visible spectrometers for measurements of stratospheric NO<sub>2</sub> for the Network for the Detection of Stratospheric Change, *J. Geophys. Res.*, 100, 16,765–16,791, 1995.
- Jaroslawski, J., and J. W. Krzyscin, Aerosol optical depth in the UV range derived from direct sun ozone observations performed by the Brewer spectrophotometer Mark II No 064 at Belsk, Poland, Atmospheric Ozone, paper presented at Quadrennial Ozone Symposium, Natl. Space Dev. Agency of Japan, Sapporo, 2000.
- Kerr, J. B., Observed dependencies of atmospheric UV radiation & trends, in *Solar Ultraviolet Radiation: Modelling, Measurements and Effects*, edited by C. S. Zerefos and A. F. Bais, *NATO ASI Ser., Ser. I*, 52, 259–266, 1997.
- Kerr, J. B., and C. T. McElroy, Evidence for large upward trends of ultraviolet-B radiation linked to ozone depletion, *Science*, 262, 1032–1034, 1993.
- Kerr, J. B., C. T. McElroy, and R. A. Olafson. Measurements of ozone with the Brewer spectrophotometer, in *Proceedings of the Quadrennial International Ozone Symposium*, edited by J. London, pp. 74–79, Natl. Cent. for Atmos. Res., Boulder, Colo., 1981.
- Kerr, J. B., W. F. J. Evans, and I. A. Asbridge. Recalibration of Dobson field spectrophotometers with a traveling Brewer spectrophotometer standard, in *Atmospheric Ozone: Proceedings of the Quadrennial Ozone Symposium Held in Halkidiki, Greece, 3–7 September 1984*, edited by C. S. Zerefos and A. Ghazi, pp. 381–386, Reidel, D., Norwell, Mass., 1985.
- Kerr, J. B., I. A. Asbridge, and W. F. J. Evans, Intercomparison of total ozone measured by the Brewer and Dobson spectrophotometers at Toronto, *J. Geophys. Res.*, 93, 11,129–11,140, 1988.
- Kerr, J. B., I. A. Asbridge, and W. F. J. Evans. Long-term intercomparison between the Brewer and Dobson spectrophotometers at Edmonton, in *Ozone in the Atmosphere: Proceedings of the Quadrennial Ozone Symposium 1988 and Tropospheric Ozone Workshop, Göttingen, Federal Republic of Germany, 4–13 August 1988*, edited by R. D. Bojkov and P. Fabian, pp. 105–108, A. Deepak, Hampton, Va., 1989.
- Kerr, J. B., C. T. McElroy, and D. I. Wardle. The Brewer instrument calibration center 1984–1996, in *Atmospheric Ozone, Proceedings of the Quadrennial Ozone Symposium*, edited by R. D. Bojkov and G. Visconti, pp. 915–918, Parco Sci. e Technol. d'Abruzzo, L'Aquila, Italy, 1998.
- Kinne, S., T. P. Akerman, M. Shiobara, A. Uchiyama, A. J. Heymsfield, L. Miloshevich, J. Wendell, E. W. Eloranta, C. Purgold, and R. W. Bergstrom, Cirrus cloud radiative and microphysical properties from ground observation and in situ measurements during FIRE 1991 and their application to exhibit problems in cirrus solar radiative transfer modeling, *J. Atmos. Sci.*, 54, 2320–2344, 1997.
- Kirchhoff, V. W. J. H., A. A. Silva, C. A. Costa, N. Paes Leme, H. G. Pavão, and F. Zaratti, UV-B optical thickness observations of the atmosphere, *J. Geophys. Res.*, 106, 2963–2973, 2001.
- Köhler, U., A comparison of the new filter ozonometer MICROTOPS II with Dobson and Brewer spectrometers at Hohenpreissenberg, *Geophys. Res. Lett.*, 26, 1385–1388, 1999.
- Molina, L. T., and M. J. Molina, Absolute absorption cross sections of ozone in the 185- to 350-nm wavelength range, *J. Geophys. Res.*, 91, 14,501–14,508, 1986.
- Solomon, S., A. L. Schmeltelopf, and R. W. Sanders, On the interpretation of zenith sky absorption measurements, *J. Geophys. Res.*, 92, 8311–8319, 1987.
- Stachelin, J., A. Renaud, J. Bader, R. McPeters, P. Viatte, B. Hoegger, V. Bugnion, M. Giroud, and H. Schill, Total ozone series at Arosa (Switzerland): Homogenization and data comparison, *J. Geophys. Res. Lett.*, 26, 5827–5841, 1998.
- VanHoosier, M. E., Solar ultraviolet spectral irradiance data with increased wavelength and irradiance accuracy, *Proc. SPIE Int. Soc. Opt. Eng.*, 2831, edited by R. E. Huffman and C. G. Stergis, 57–64, 1996.
- Vanicek, K., Differences between Dobson and Brewer observation of total ozone at Hradec Kralove, in *Atmospheric Ozone, Proceedings of the Quadrennial Ozone Symposium*, edited by R. D. Bojkov and G. Visconti, pp. 81–84, Parco Sci. e Technol. d'Abruzzo, L'Aquila, Italy, 1998.
- Vanier, J., and D. I. Wardle, The effects of spectral resolution in total ozone measurements, *Q. J. R. Meteorol. Soc.*, 95, 395–399, 1969.
- Wardle, D. I., C. T. McElroy, J. B. Kerr, E. Wu, and K. Lamb. Laboratory tests on the double dispersing Brewer spectrophotometer, in *Atmospheric Ozone, Proceedings of the Quadrennial Ozone Symposium*, edited by R. D. Bojkov and G. Visconti, pp. 997–1000, Parco Sci. e Technol. d'Abruzzo, L'Aquila, Italy, 1998.
- Weatherhead, E., et al., Temperature dependence of the Brewer ultraviolet data, *J. Geophys. Res.*, 106, 34,121–34,129, 2001.

J. B. Kerr, Meteorological Service of Canada, Environment Canada, 4905 Dufferin Street, Downsview, Ontario, Canada M3H 5T4. (kerr@ec.gc.ca)